Advanced Analytical Chemistry

Week 05

Surface analysis

Department of Applied Chemistry
Prof. Chan Woo Lee

How to obtain information of analyte ?

- To retrieve the desired information from the analyte, it is necessary to provide a stimulus, which is usually in the form of electromagnetic, electrical, mechanical, or nuclear energy

- The resulting information is contained in the phenomena that result from the interaction of the stimulus with the analyte.

- The stimulus elicits a response from the system under study whose nature and magnitude are governed by the fundamental laws of chemistry and physics.

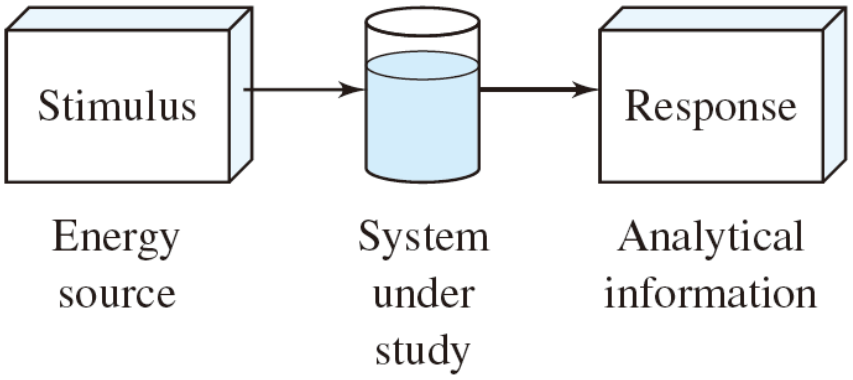

FIGURE 1-1 Block diagram showing the overall process of an instrumental measurement.

D. A. Skoog, Principles of Instrumental Analysis, 7th Ed., Cengage Learning, 2017, p. 3

Importance of surface chemistry

- All solid materials interact with their surroundings through their surfaces.
- The surface composition and structure determines the nature of interactions.

- Surfaces, therefore, influence many important properties of the solid.

(ex) corrosion, catalytic activity, adhesive properties, wettability, contact potential, etc.

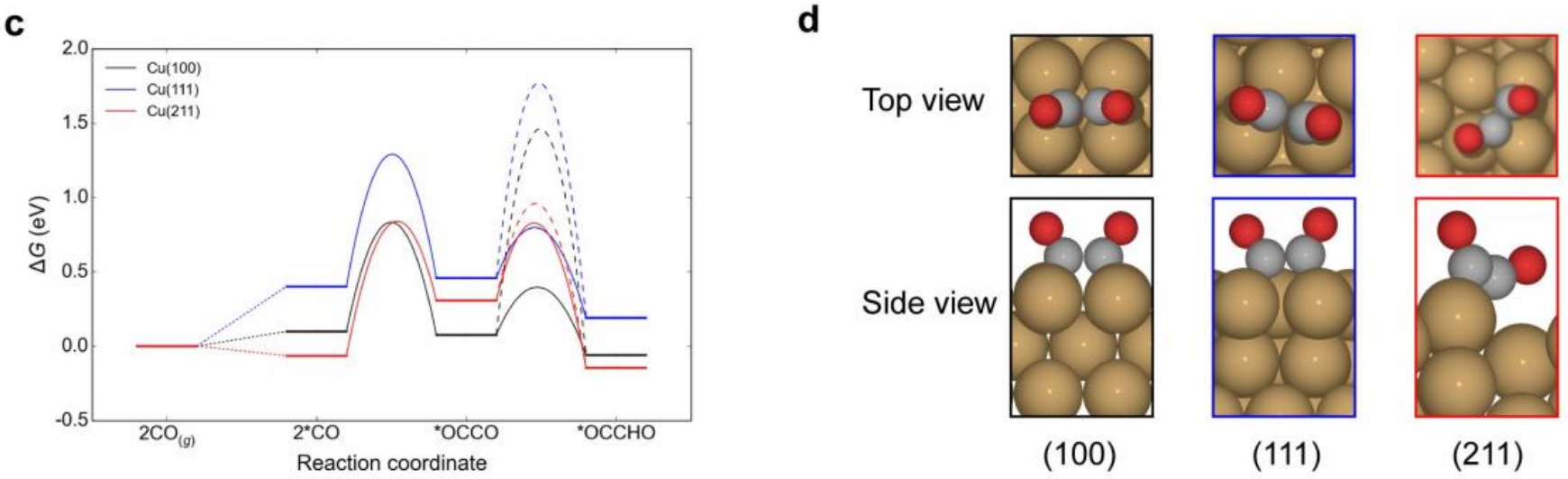

DFT simulations of C-C coupling on Cu facets. (c) Free energy diagram at 0 V (RHE) for the energetics of the dimerization of *CO to form *OCCO and the subsequent surface hydrogenation (solid lines) and proton-electron transfer (dashed lines) to form *OCCHO in the presence of a solvent and cation-induced field (d) *OCCO configurations on the (100), (111) and (211) facets, where solvent molecules have been removed to show the adsorbate configurations.

C–C coupling reactions are favored on the Cu(211) and Cu(100) surfaces than Cu(111)

https://doi.org/10.1038/s41929-017-0009-x (22.09.16)

What is the surface ?

- Usually, **the range of 'surface' is defined differently** by scientists:

(1) the top monolayer, (2) the first ten or so layers (<2-3 nm)
(3) the surface film, no greater than 100 nm.

- 'surface' is regarded as a part of material **different from bulk regions.**

- **Surface analysis requires really high surface sensitivity !**

(ex) In a Ni cube of 1 cm^3, total atoms # = ~10^{23}. / surface atom # = ~10^{16}
The ratio of surface atoms is ~ $1/10^7$ (e.g. 100 ppb)
(ex) In a 1% Cu-doped Ni cube, the Cu concentration ~ 1 ppb

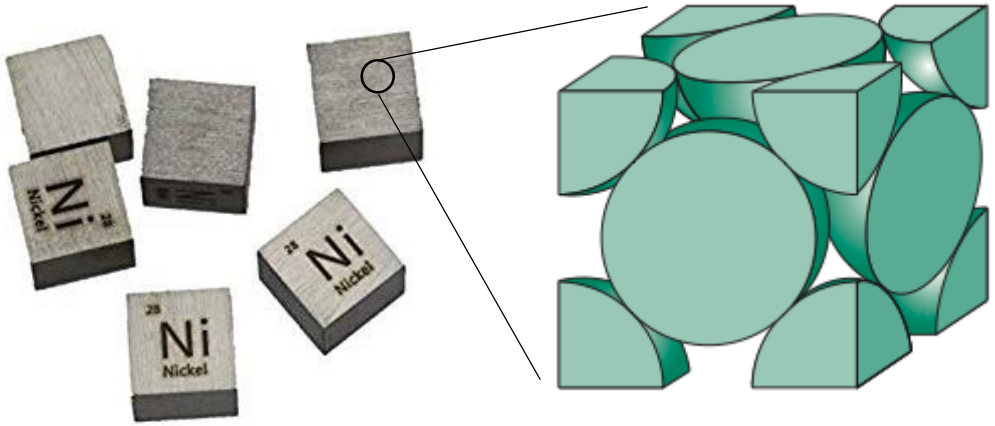

Face-centered cubic
4 atoms per unit cell
a_0 = 0.352 nm

$$N = \frac{1cm^3}{(0.352\,nm)^3} \times 4 = \sim 10^{23} \qquad N_s = \frac{1cm^2}{(0.352\,nm)^2} \times 4 \times 6 = \sim 2 \times 10^{16}$$

DOI:10.13140/RG.2.2.27679.79522 (22.09.16)

Surface analysis techniques

- Topography: the surface shape and features of an area
- SEM (scanning electron microscopy), STM (Scanning tunneling microscope)
- XPS (X-ray photoelectron spectroscopy), ESCA (Electron spectroscopy for chemical analysis)
- AES (Auger electron spectroscopy), SIMS (Secondary-ion mass spectrometry)

Table 1.1 Surface analysis techniques and the information they can provide

Radiation IN Radiation DETECTED	photon electron	photon photon	electron electron	ion ion	neutron neutron
SURFACE INFORMATION					
Physical topography			SEM STM (9)		
Chemical composition	ESCA/XPS (3)		AES (2)	SIMS (5) ISS (6)	
Chemical structure	ESCA/XPS (3)	EXAFS (8) IR & SFG (7)	EELS (7)	SIMS (4)	INS (7)
Atomic structure		EXAFS (8)	LEED RHEED (8)	ISS (6)	
Adsorbate bonding		EXAFS (8) IR (7)	EELS (7)	SIMS (4)	INS (7)

J. C. Vickerman, Surface Analysis-The principal Techniques, 2nd Ed., John Wiley & Sons, Ltd., 2009, p. 4

Energy of light

Molar heat of vaporization for water = 40.7 kJ/mol

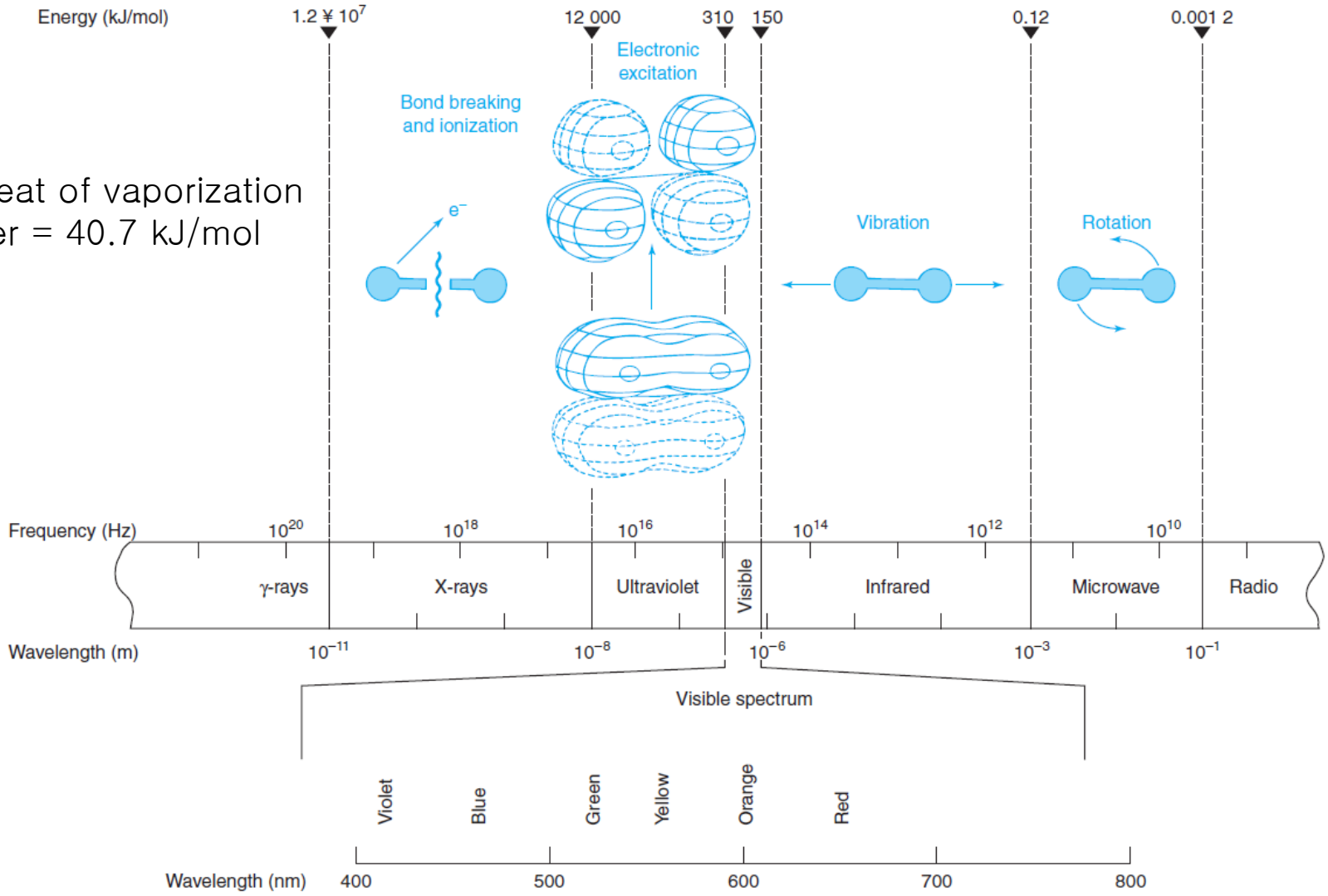

FIGURE 18-2 Electromagnetic spectrum, showing representative molecular processes that occur when light in each region is absorbed. The visible spectrum spans the wavelength range 380–780 nanometers (1 nm = 10^{-9} m).

D. C. Harris, Quantitative Chemical Analysis, 9th Ed., W. H. Freeman, 2015, p. 434

X-ray photoelectron spectroscopy

- Photoelectric effect: emission of electron when lights hit a material
- X-ray photons ($E = h\nu$) displaces an electron from a K orbital of energy E_b

An atom, molecule or ion

$$A + h\nu \rightarrow A^{+*} + e^-$$

Emitted e^-

X-ray

the electronically excited with a more positive charge

The **kinetic energy** of the emitted electron E_k is measured in an electron spectrometer. The **binding energy** of the electron E_b can then be calculated.

$$E_b = h\nu - E_k - w$$

*where **w** is the work function of the spectrometer, a factor that corrects for the electrostatic environment in which the electron is formed and measured.*

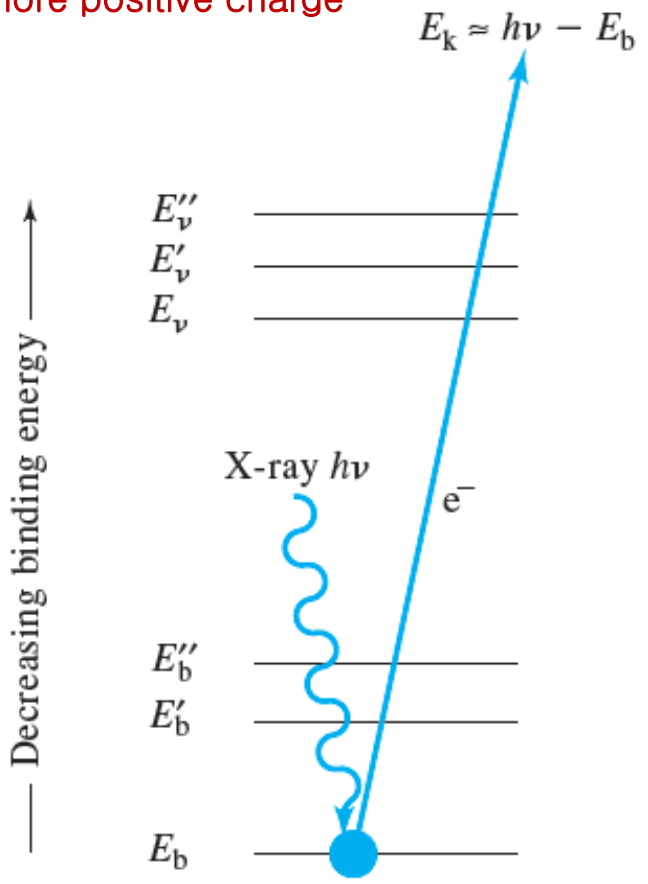

E_b, E_b', and E_b'' represent binding energies of the inner-shell K and L electrons of an atom. The upper three lines represent some of the energy levels of the outer shell, or valence electrons.

D. A. Skoog, Principles of Instrumental Analysis, 7th Ed., Cengage Learning, 2017, p. 541

X-ray photoelectron spectroscopy

$$E_k = h\nu - E_b - \phi_{sample}$$

$$E_k = h\nu - E_b - \phi_{sample} - (\phi_{sp} - \phi_{sample}) = h\nu - E_b - \phi_{sp}$$

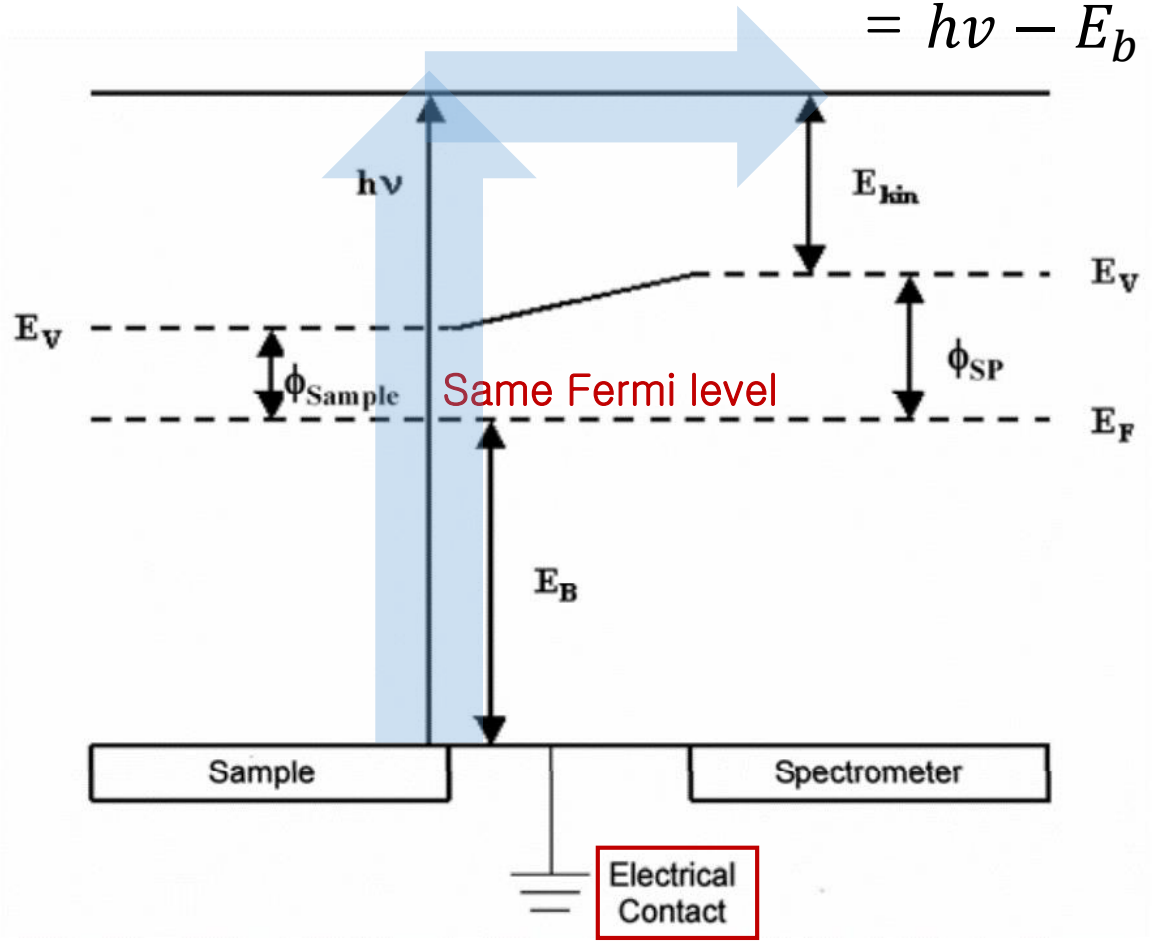

https://doi.org/10.1116/6.0000412 (22.09.16)

Other processes derived from X-ray

(1) By exposing the analyte to X-ray, the excitation process occur, losing e^-

$$A + \underbrace{h\nu}_{\text{X-ray}} \rightarrow A^{+*} + \underbrace{e^-}_{\text{Emitted } e^-}$$

(2) relaxation of the excited ion $A^{+}*$ can occur

$$A^{+*} \rightarrow A^{++} + e_A^-$$

Auger e^-

$$A^{+*} \rightarrow A^{+} + h\nu$$

X-ray fluorescence

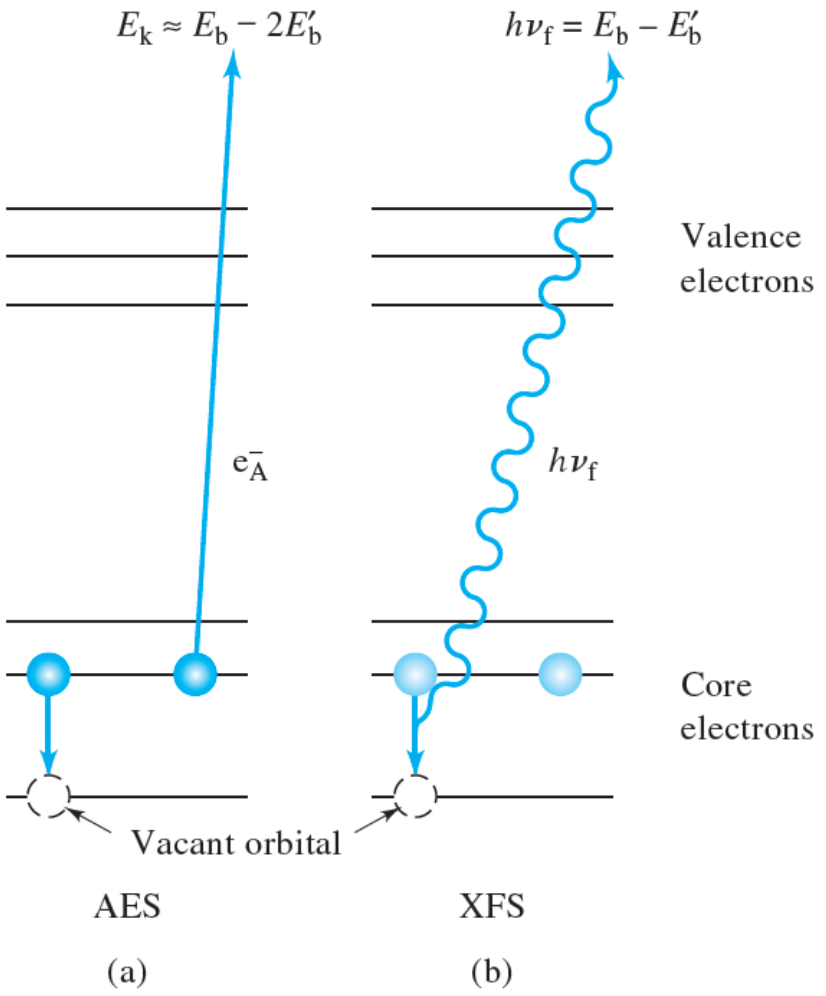

FIGURE 21-7 Schematic representation of the source of (a) Auger electron emission and (b) X-ray fluorescence that competes with Auger emission.

D. A. Skoog, Principles of Instrumental Analysis, 7th Ed., Cengage Learning, 2017, p. 545

Instrumentation of XPS

X-ray emission of Al K_α

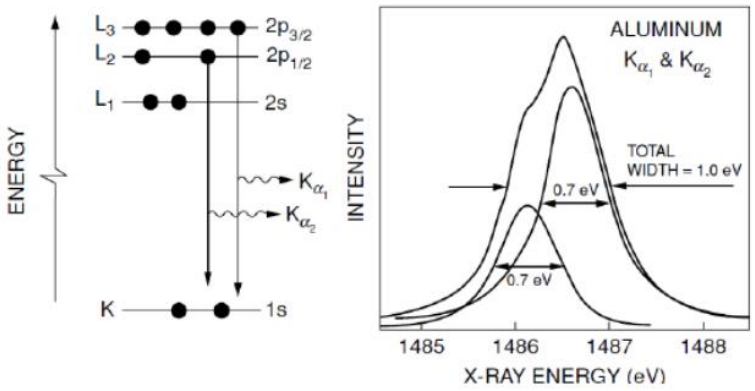

Anode	Line	Energy (eV)	Width (eV)
Mg	K_α	1253.6	0.7
Al	K_α	1486.6	0.85
Si	K_α	1739.5	1.0
Zr	L_α	2042.4	1.7
Ag	L_α	2984	2.6
Ti	K_α	4510	2.0
Cr	K_α	5415	2.1

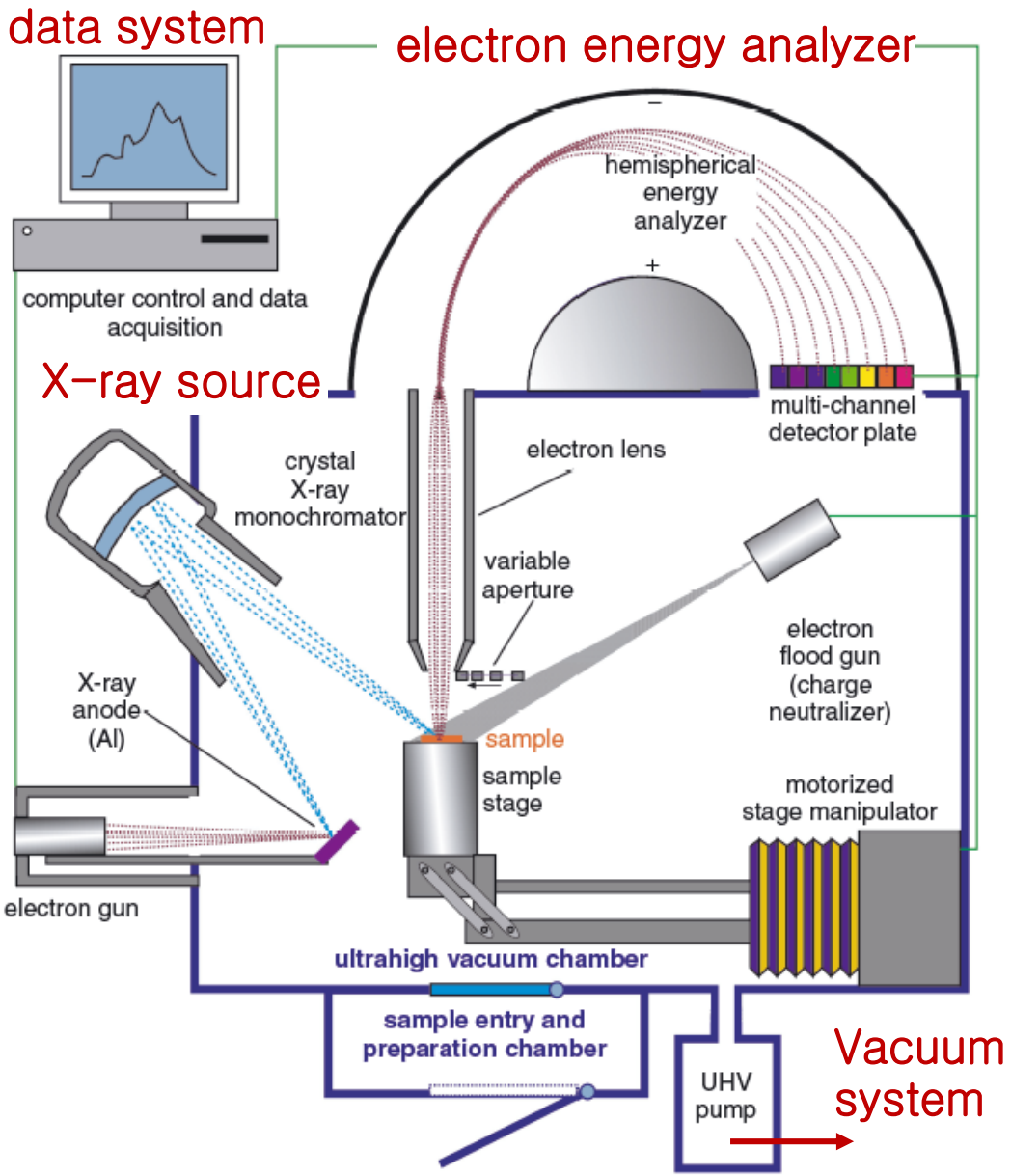

Vaccum inhibits the collison of electrons and surface composition change

J. C. Vickerman, Surface Analysis-The principal Techniques, 2nd Ed., John Wiley & Sons, Ltd., 2009, p. 81

Sampling depth

- Sampling depth where e⁻ are emitted is limited at surface due to inelastic scattering

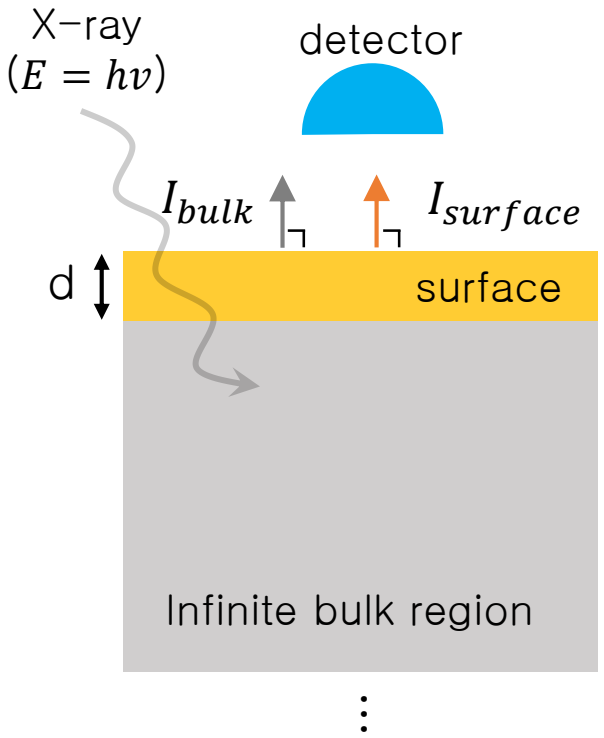

I_∞ = e⁻ signal without energy loss from all depths
$= I_{bulk} + I_{surface}$

$$I_{bulk} = I_\infty \, exp\left(-\frac{d}{\lambda}\right)$$

$$I_{surface} = I_\infty \left[1 - exp\left(-\frac{d}{\lambda}\right)\right]$$

e⁻ signals without energy loss

63.3% from the surface with **d = λ**
86.4% from the surface with **d = 2λ**
95.0% from the surface with **d = 3λ**

Sampling depth

- IMFP (**inelastic mean free path, λ**): the average distance that an e⁻ with a given energy travels between successive inelastic collisions
- Depends on the kinetic energy of e⁻ and the nature of samples

$$\text{IMFP} = \lambda = 538\text{KE}^{-2} + 0.41(a\text{KE})^{0.5} \quad \text{(for elements)}$$
$$\text{IMFP} = \lambda = 2170\text{KE}^{-2} + 0.72(a\text{KE})^{0.5} \quad \text{(for inorganic compounds)}$$
$$\text{IMFP} = \lambda_d = 49\text{KE}^{-2} + 0.11\text{KE}^{0.5} \quad \text{(for organic compounds)}$$

Sampling depth

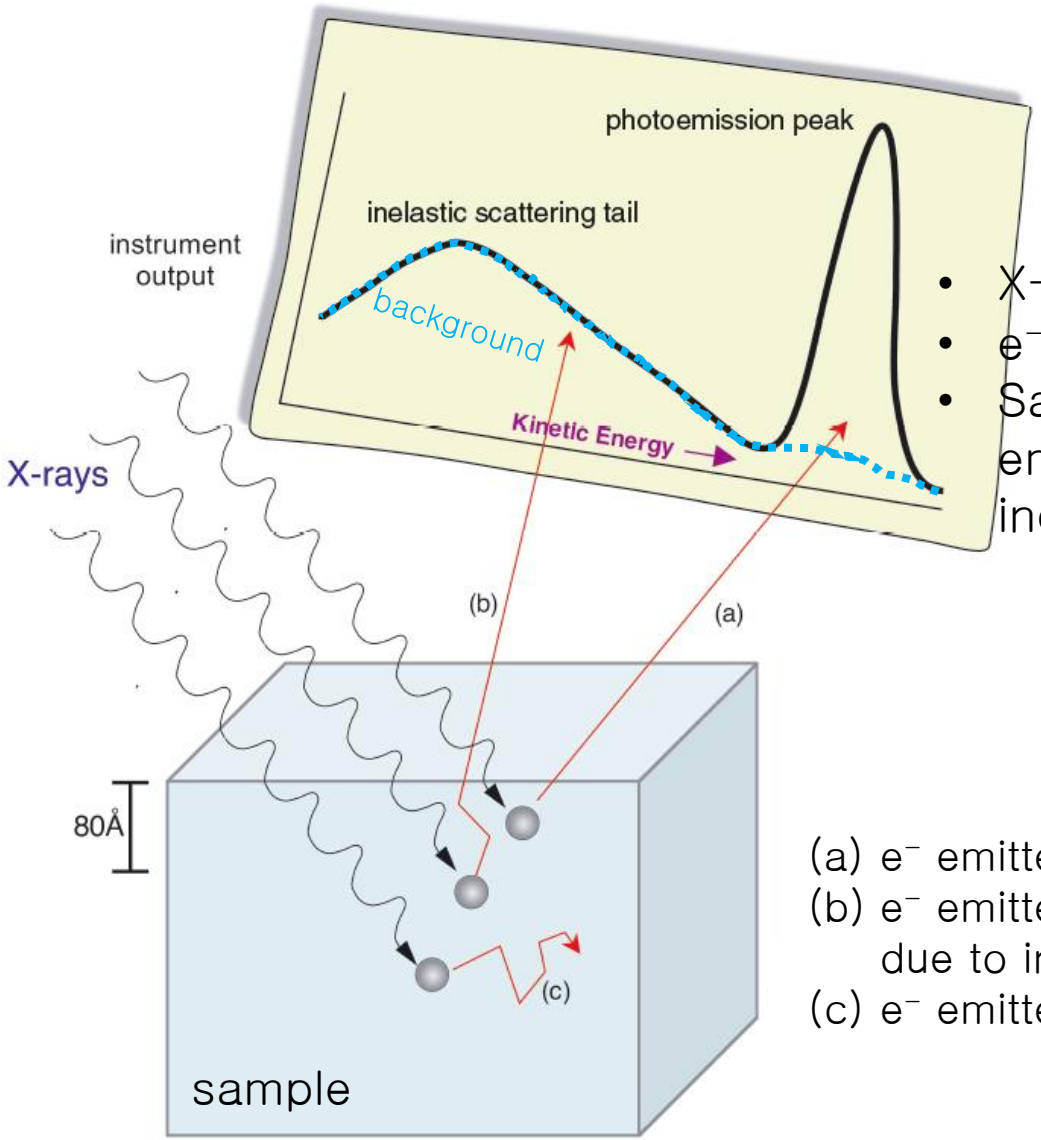

- X-ray penetration depth: > 1μm
- e^- escaping depth : ~5 nm for 1 keV
- Sampling depth where e^- are emitted is limited at surface due to inelastic scattering

(a) e^- emitted from surface without energy loss
(b) e^- emitted from surface with some energy loss due to inelastic interactions
(c) e^- emitted from a deep region within a sample

J. C. Vickerman, Surface Analysis-The principal Techniques, 2nd Ed., John Wiley & Sons, Ltd., 2009, p. 64

Electron energy analyzer

- Analyzer system: collection lens, energy analyzer, detector
- **Collection lens:** collect photoelectrons and **slow down electrons** as energy set
  ex) 190 eV → 90 eV, **150 eV → 50 eV**, 110 eV → 10 eV, 80 eV → −20 eV (X)
- **Energy analyzer:** changes the pathway of electrons by an electrostatic field
- **Pass energy:** the electron energy for successful arrival of electron into detector

Electrostatic hemispherical analyzer

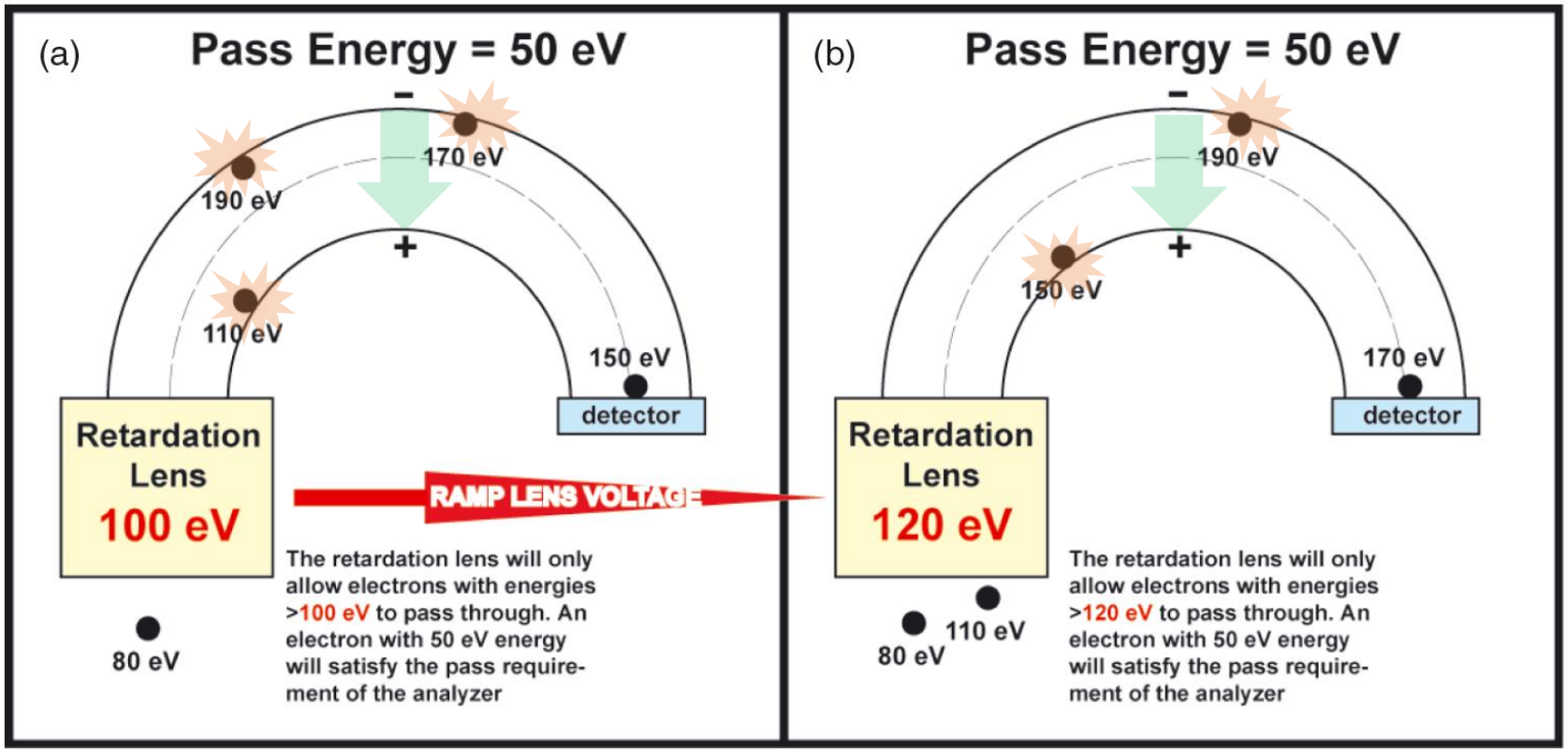

Entire XPS spectrum is acquired by ramping lens voltages with the pass energy fixed

J. C. Vickerman, Surface Analysis-The principal Techniques, 2nd Ed., John Wiley & Sons, Ltd., 2009, p. 87

X선 광전자 분광기 | XPS

전체장비목록

XPS-ESCA

위 치 : 산학관 106호
Maker : VG microtech
Model : ESCA 2000

담당자 : 류원택
이메일 : ryuwt@kookmin.ac.kr
연락처 : 02-910-4838

점검중
로그인후 신청가능

장비정보 | 분석의뢰현황 | 공지사항 | Q&A

Equipment
X-rayphotoelectron spectrometer (XPS)

Maker
VG microtech

Model
ESCA2000 ESCA (Electron spectroscopy for chemical analysis)

Spec
- CHA type (ConcentricHemispherical analyzer)
- Energy analysis range (0 - 2500eV)
- Peak sensitivity
- 0.85eV resolution :800,000cps
- 1.00eV resolution : 4,500,000cps
- 1.40eV resolution : 11,000,000cps
- Twin anode x-ray source (Mg/Al)

Application
비 파괴, 표면성분원소의 확인정량 ;Chemical shift 측정에의한 결정상태 규명,Work function 측정

Possible information from XPS

Table 3.1 Information derived from an ESCA experiment

In the outermost 10 nm of a surface, ESCA can provide the following:

- Identification of all elements (except H and He) present at concentrations >0.1 atomic %.
- Semiquantitative determination of the approximate elemental surface composition (error $< \pm 10\%$).
- Information about the molecular environment (oxidation state, covalently bonded atoms, etc.).
- Information about aromatic or unsaturated structures or paramagnetic species from shake-up ($\pi^* \rightarrow \pi$) transitions.
- Identification of organic groups using derivatization reactions.
- Non-destructive elemental depth profiles 10 nm into the sample and surface heterogeneity assessment using (1) angular-dependent ESCA studies and (2) photo-electrons with differing escape depths.
- Destructive elemental depth profiles several hundred nanometers into the sample using ion etching.
- Lateral variations in surface composition (spatial resolutions down to 5 μm for laboratory instruments and spatial resolutions down to 40 nm for sychrotron-based instruments).
- 'Fingerprinting' of materials using valence band spectra and identification of bonding orbitals.
- Studies on hydrated (frozen) surfaces.

J. C. Vickerman, Surface Analysis-The principal Techniques, 2nd Ed., John Wiley & Sons, Ltd., 2009, p. 50

Qualitative identification of elements

- All elements except H and He emit core electrons with characteristic E_B.
- E_B for 1s e^- increases with Z due to the **higher (+) charge** of the nucleus.
- The closer the electron is to the nucleus, the higher E_B they have.

plot of electron-counting rate as a function of binding energy E_B

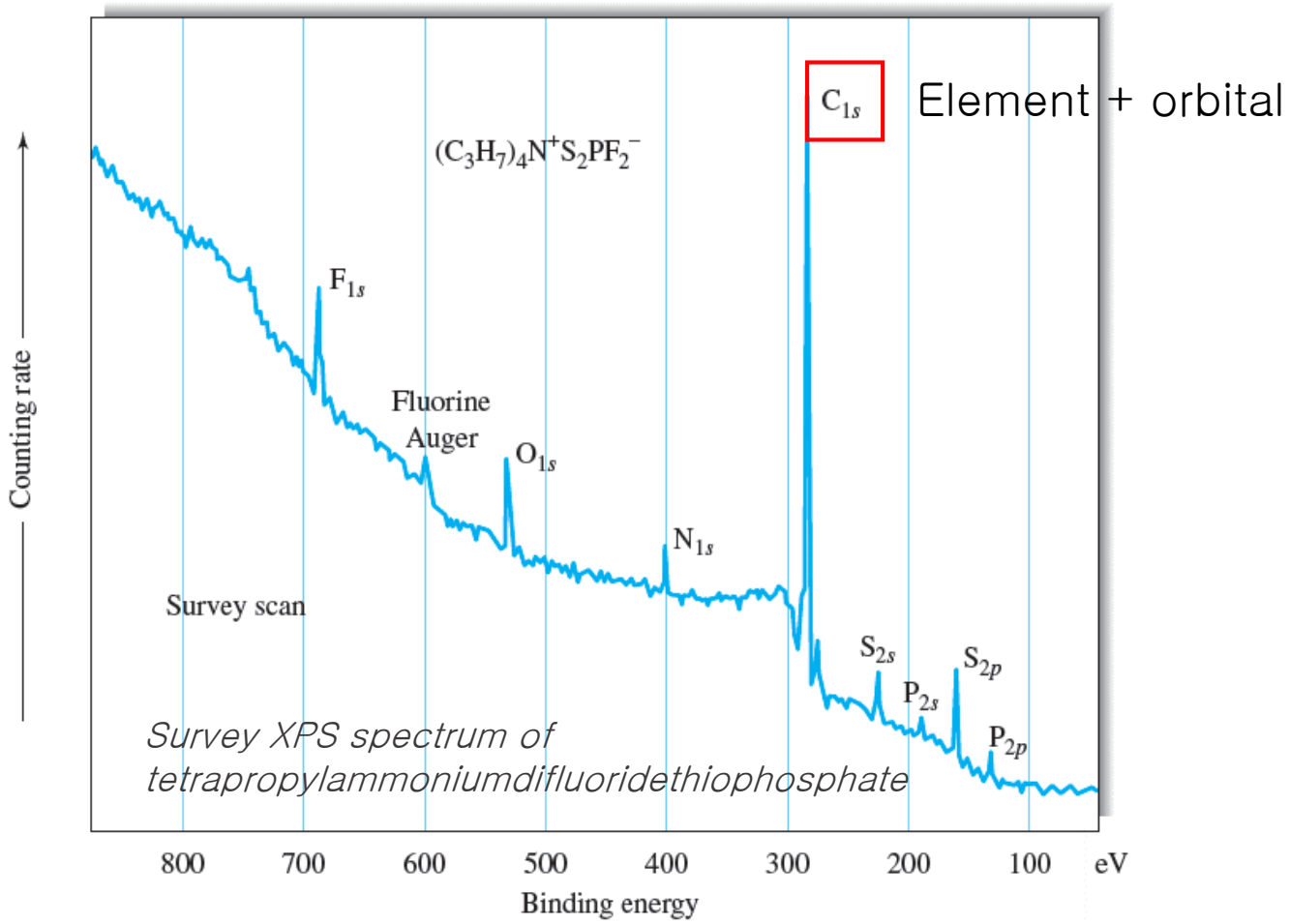

D. A. Skoog, Principles of Instrumental Analysis, 7th Ed., Cengage Learning, 2017, p. 541

Chemical shifts and Oxidation states

- The peak position depends on the chemical environment of the atom responsible for the peak. That is, variations in the number of valence electrons, and the type of bonds they form, influence the binding energies of core electrons.

- Binding energies increase as the oxidation state becomes more positive. When one of these electrons is removed, the effective charge sensed for the core electron is increased, and an increase in binding energy results.

TABLE 21-2 Chemical Shifts as a Function of Oxidation State[a]

Element[b]	Oxidation State									
	−2	−1	0	+1	+2	+3	+4	+5	+6	+7
Nitrogen (1*s*)	—	*0[c]	—	+4.5[d]	—	+5.1	—	+8.0	—	—
Sulfur (1*s*)	−2.0	—	*0	—	—	—	+4.5	—	+5.8	—
Chlorine (2*p*)	—	*0	—	—	—	+3.8	—	+7.1	—	+9.5
Copper (1*s*)	—	—	*0	+0.7	+4.4	—	—	—	—	—
Iodine (4*s*)	—	*0	—	—	—	—	—	+5.3	—	+6.5
Europium (3*d*)	—	—	—	—	*0	+9.6	—	—	—	—

[a]All shifts are in electron volts measured relative to the oxidation states indicated by (*). (Reprinted with permission from D. M. Hercules, *Anal. Chem.*, **1970**, *42*, 20A, **DOI**: 10.1021/ac60283a717. Copyright 1970 American Chemical Society.)

[b]Type of electrons given in parentheses.

[c]Arbitrary zero for measurement, end nitrogen in NaN_3.

[d]Middle nitrogen in NaN_3.

D. A. Skoog, Principles of Instrumental Analysis, 7th Ed., Cengage Learning, 2017, p. 543

Photoelectric process

$$E_B = E_f(n-1) - E_i(n)$$

$$E_B = -\varepsilon_k - E_r(K) - (\delta\varepsilon_{corr} + \delta\varepsilon_{rel})$$

E_B = binding energy

$E_i(n)$ = the energy of the initial state with n electrons

$E_f(n-1)$ = the energy of the final state with n−1 electrons

ε_k = orbital energy of the ejected photoelectron at the initial state

$E_r(K)$ = relaxation energy, $\delta\varepsilon_{corr} + \delta\varepsilon_{rel}$ = correction factors, typically neglible

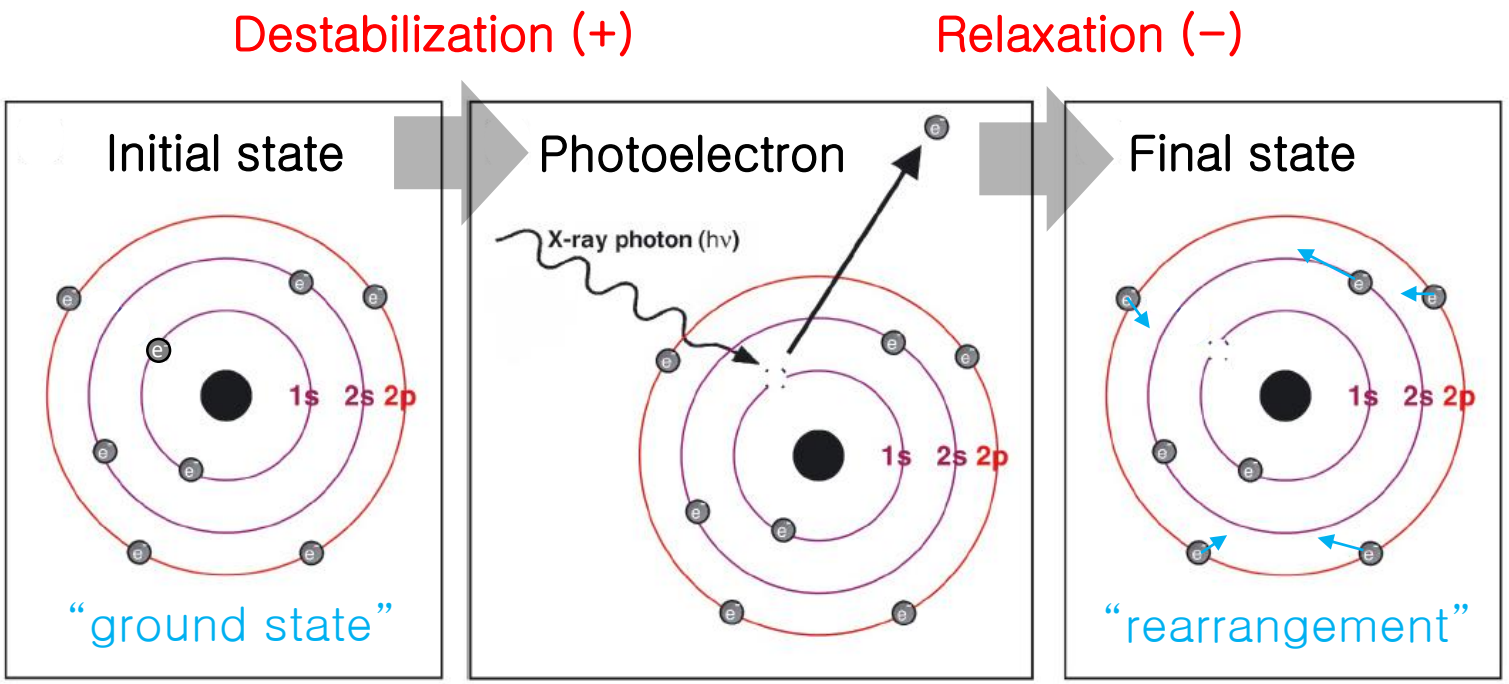

J. C. Vickerman, Surface Analysis-The principal Techniques, 2nd Ed., John Wiley & Sons, Ltd., 2009, p. 52

Initial state effects

- **Initial state effect:** the change of initial state leads to the change of E_B

For most samples, relaxation effect is similar although initial state is changed:

Chemical shift: $\Delta E_B = -\Delta\varepsilon_k - \Delta E_r(K)$

e.g., the changes in the distribution and density of electrons of an atom resulting from changes in its chemical environment contribute to ΔE_B

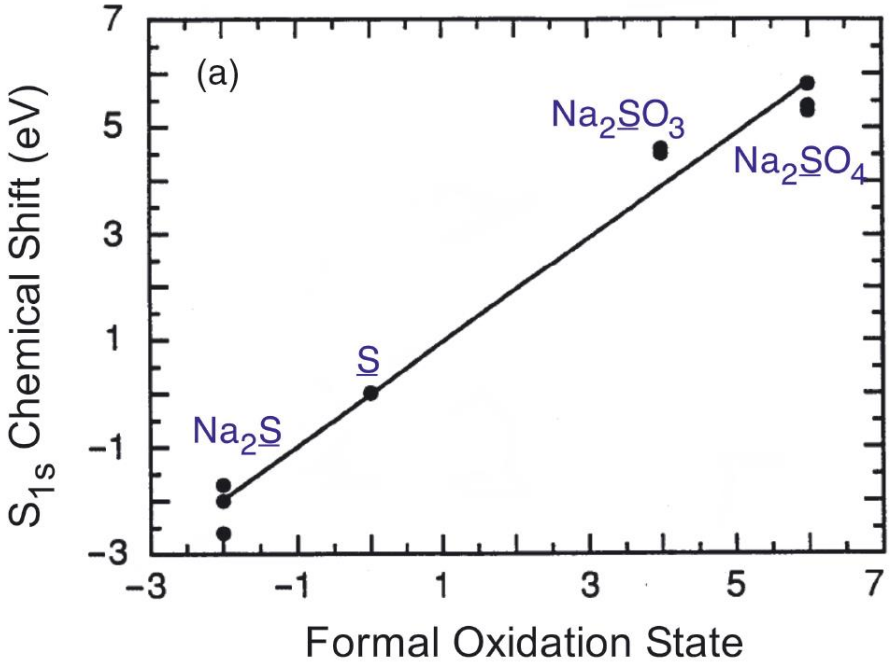

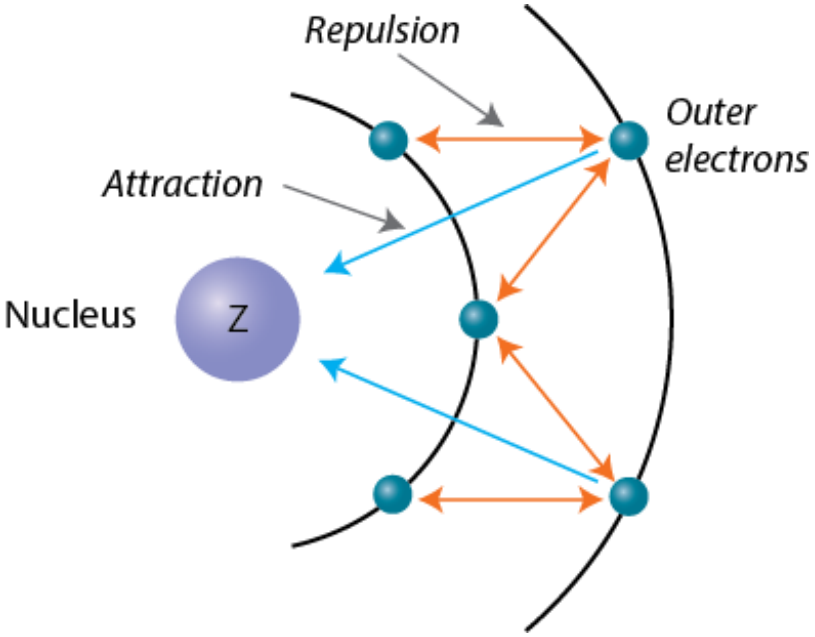

J. C. Vickerman, Surface Analysis-The principal Techniques, 2nd Ed., John Wiley & Sons, Ltd., 2009, p. 55

https://thefactfactor.com/tag/electron-affinity (22.09.16)

Initial state effects

- The C 1s E_B increases as the number of O bonded to C increases since O is more electronegative and draws electrons from C

Table 3.2 Typical C_{1s} binding energies for organic samples[a]

Functional group		Binding energy (eV)
Hydrocarbon	C—H, C—C	285.0
Amine	C—N	286.0
Alcohol, ether	C—O—H, C—O—C	286.5
Cl bound to carbon	C—Cl	286.5
F bound to carbon	C—F	287.8
Carbonyl	C=O	288.0
Amide	N—C=O	288.2
Acid, ester	O—C=O	289.0
Urea	N—C(=O)—N	289.0
Carbamate (urethane)	O—C(=O)—N	289.6
Carbonate	O—C(=O)—O	290.3
2F bound to carbon	—CH_2CF_2—	290.6
Carbon in PTFE	—CF_2CF_2—	292.0
3F bound to carbon	—CF_3	293–294

Ethyl trifluoroacetate

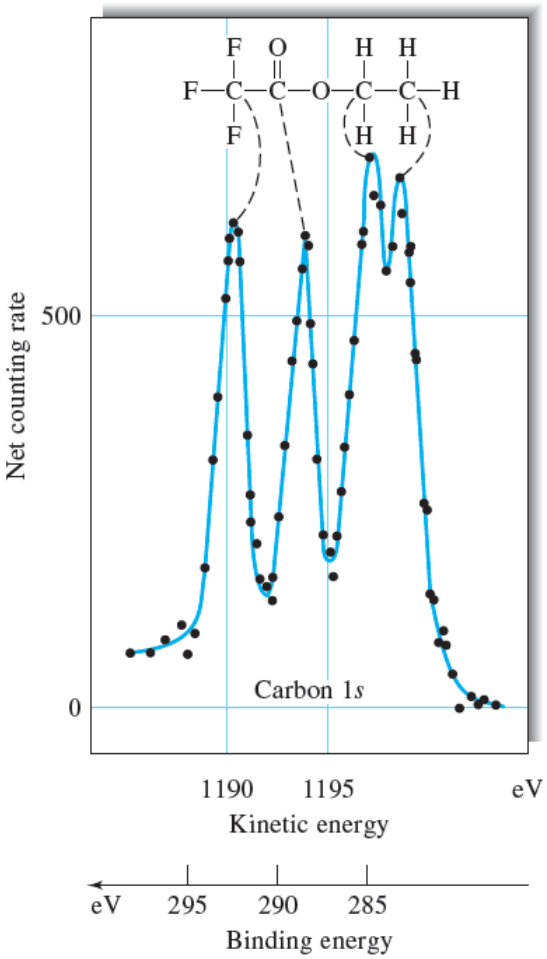

D. A. Skoog, Principles of Instrumental Analysis, 7th Ed., Cengage Learning, 2017, p. 544

J. C. Vickerman, Surface Analysis-The principal Techniques, 2nd Ed., John Wiley & Sons, Ltd., 2009, p. 56

Charge potential model

- The formal oxidation state is not exactly correlated with ΔE_B
- the formal oxidation state is effective only when the chemical bonding is completely ionic.
- ΔE_B is much more correlated with the charge imposed on the atom

$$E_B = E_B^\circ + kq_i + \sum_{j \neq i} \frac{q_j}{r_{ij}} \rightarrow V_i$$

$$\Delta E_B = k\Delta q_i + \Delta V_i$$

E_B = binding energy
E_B° = a reference energy of the neutral atom
q_i = the charge on atom i
q_j = the charge on the surrounding atoms j at distance r_{ij} (opposite sign to q_i)
ΔV_i = the potential change in the surrounding atoms
k = constant

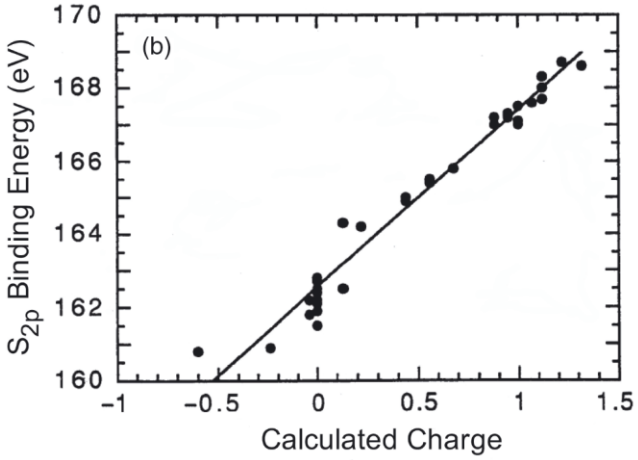

As the positive charge on the atom increases by formation of chemical bonds, E_B will increase.

J. C. Vickerman, Surface Analysis-The principal Techniques, 2nd Ed., John Wiley & Sons, Ltd., 2009, p. 55

Spin–orbit splitting

- **Spin–orbit splitting:** All orbital levels except for s levels (l = 0) give rise to **a doublet** with the two possible states having **different binding energies** "initial state effect"
- Spin and orbital motion of e^- make magnetic moments interacting with each other.

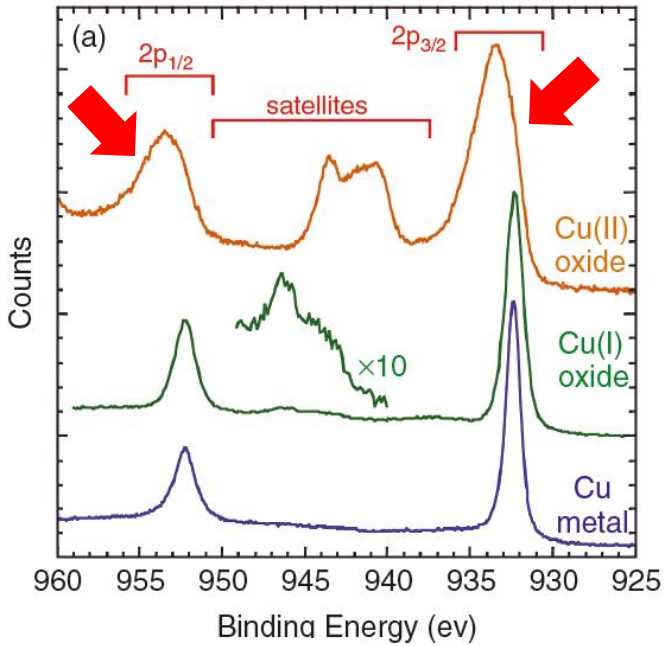

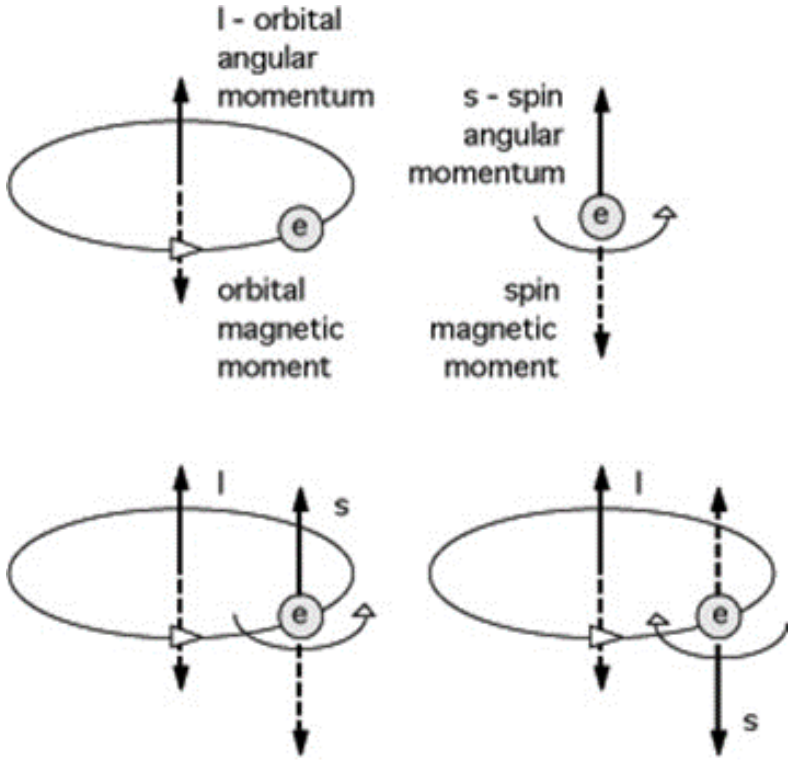

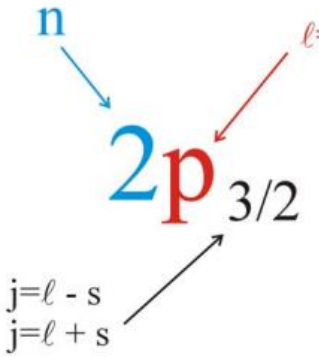

n : the principal quantum number
l : the angular momentum quantum number
s : the spin angular momentum number ($\pm\frac{1}{2}$)
j : total angular momentum quantum number

J. C. Vickerman, Surface Analysis-The principal Techniques, 2nd Ed., John Wiley & Sons, Ltd., 2009, p. 57

Nomenclature

Table 1.2 The relationship between quantum numbers, spectroscopists' notation and X-ray notation

Quantum numbers				Spectroscopists' notation	X-ray notation
n	l	s	j		
1	0	$+1/2, -1/2$	1/2	$1s_{1/2}$	K
2	0	$+1/2, -1/2$	1/2	$2s_{1/2}$	L_1
2	1	$+1/2$	1/2	$2p_{1/2}$	L_2
2	1	$-1/2$	3/2	$2p_{3/2}$	L_3
3	0	$+1/2, -1/2$	1/2	$3s_{1/2}$	M_1
3	1	$+1/2$	1/2	$3p_{1/2}$	M_2
3	1	$-1/2$	3/2	$3p_{3/2}$	M_3
3	2	$+1/2$	3/2	$3d_{3/2}$	M_4
3	2	$-1/2$	5/2	$3d_{5/2}$	M_5
					etc.

J. F. Watts, An Introduction to Surface Analysis by XPS and AES, 1st Ed., John Wiley & Sons Ltd, 2003, p. 5

Final state effects

- **final state effect:** The electron rearrangements that occur during photoemission result in **higher KE** and **lower E_B**.
- **Source:** mainly rearrangement of outer shell electrons with smaller E_B than the emitted.

Chemical shift: $\Delta E_B = \underbrace{-\Delta\varepsilon_k}_{(+)} \underbrace{-\Delta E_r(K)}_{(-)}$

(ex) Co $2p_{3/2}$ E_B : Co^0 (778.2 eV) < Co^{3+} (779.6 eV) < Co^{2+} (780.5 eV)
Cu $2p_{3/2}$ E_B: Cu^0 and Cu^+ (932.5 eV)

Cu 2p

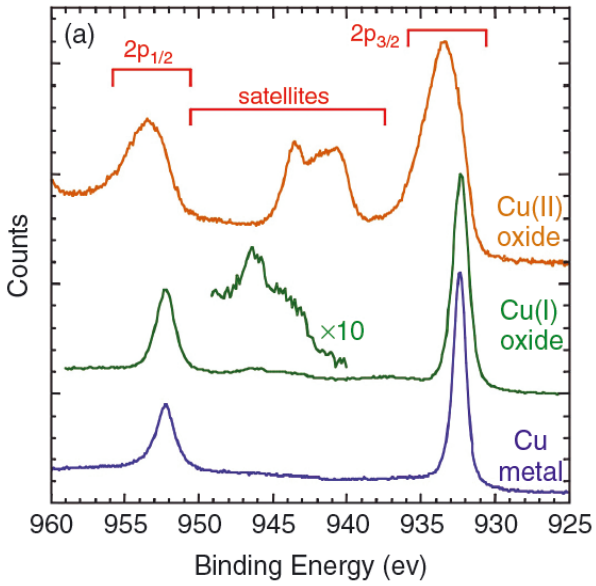

Cu Auger LVV

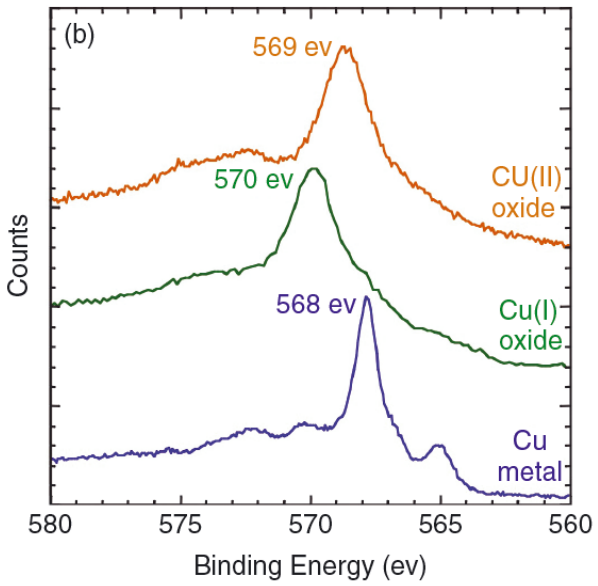

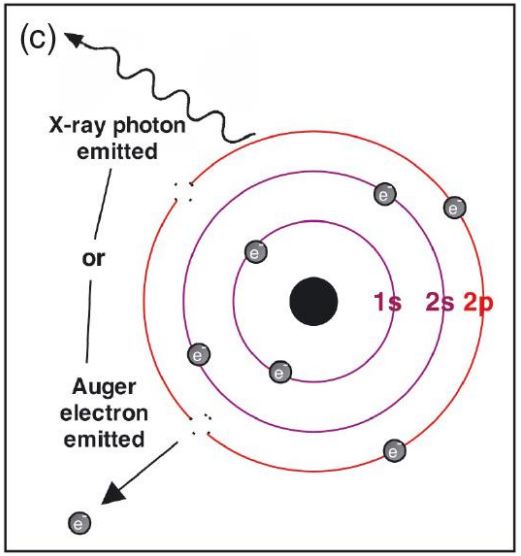

J. C. Vickerman, Surface Analysis-The principal Techniques, 2nd Ed., John Wiley & Sons, Ltd., 2009, p. 57, p. 52

Shake-up/off satellites

- Photoemission can leave ions in the ground state as well as in an excited state, the latter causes the **lower KE** of photoelectrons, therefore **higher E_B**

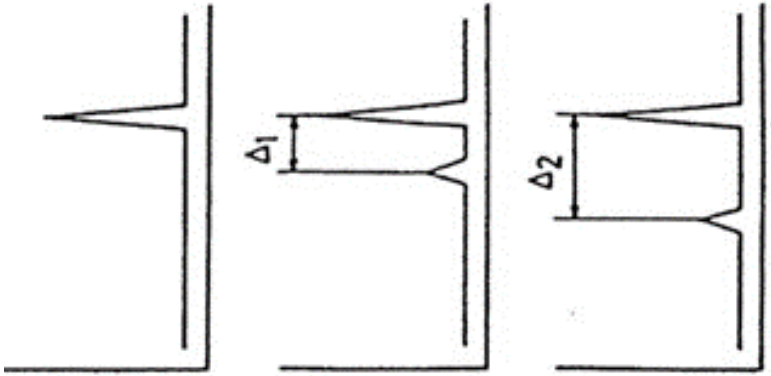

- **Shake-up:** excitation of e^- to bound state
- **shake-off:** excitation of e^- to unbound state

"final state effect"

Many transition metal oxides have unique shake-up features which can be used to analyze the chemical state

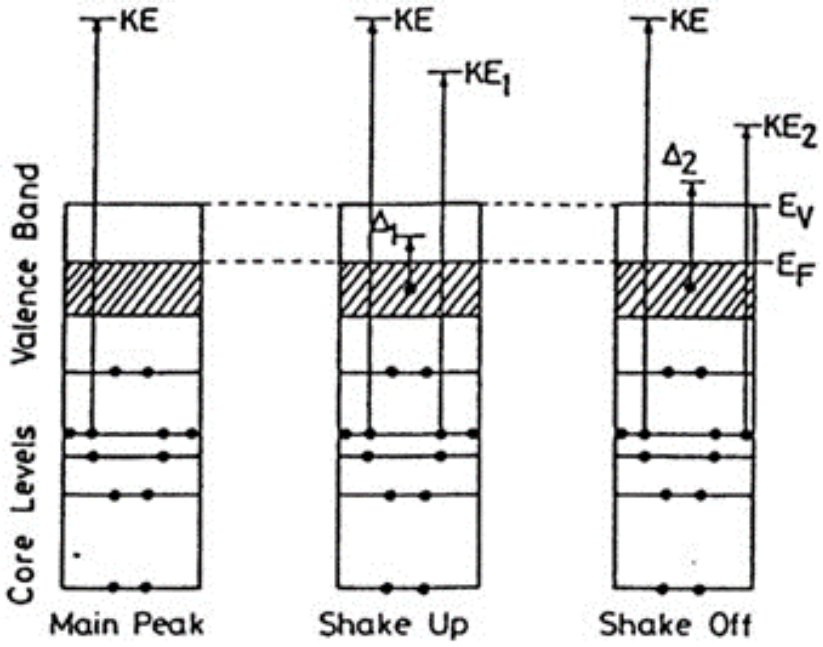

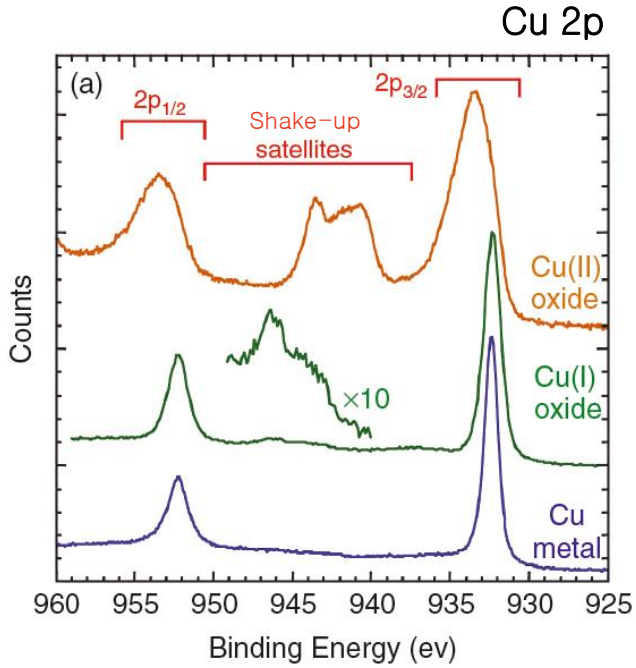

https://slideplayer.com/slide/4700446/ (22.09.16)

J. C. Vickerman, Surface Analysis-The principal Techniques, 2nd Ed., John Wiley & Sons, Ltd., 2009, p. 57

Quantification

-If the solid is homogeneous, we can express the number of photoelectrons detected per second, I:

$$I = n\phi\sigma\varepsilon\eta A T l$$

n = the number density of atoms (atoms/cm^3) in the sample
ϕ = the flux of the incident X-ray beam (photons/cm^2 s)
σ = the photoelectric cross section for the transition (cm^2/atom)
ε = the angular efficiency factor for the instrument
η = the efficiency of producing photoelectrons (photoelectrons/photon)
A = analysis area of the sample (cm^2)
T = the efficiency of detector
l = the mean free path of the photoelectrons in the sample (cm)

For a given transition, the last six terms are constant, and we can write the atomic sensitivity factor S as:

$$S = \sigma\varepsilon\eta A T l$$

The ratio I/S is directly proportional to the concentration n on the surface.
I = peak area.

$$Atomic\ \% = \frac{I_A/S_A}{\sum I_i/S_i} \times 100$$

Quantification

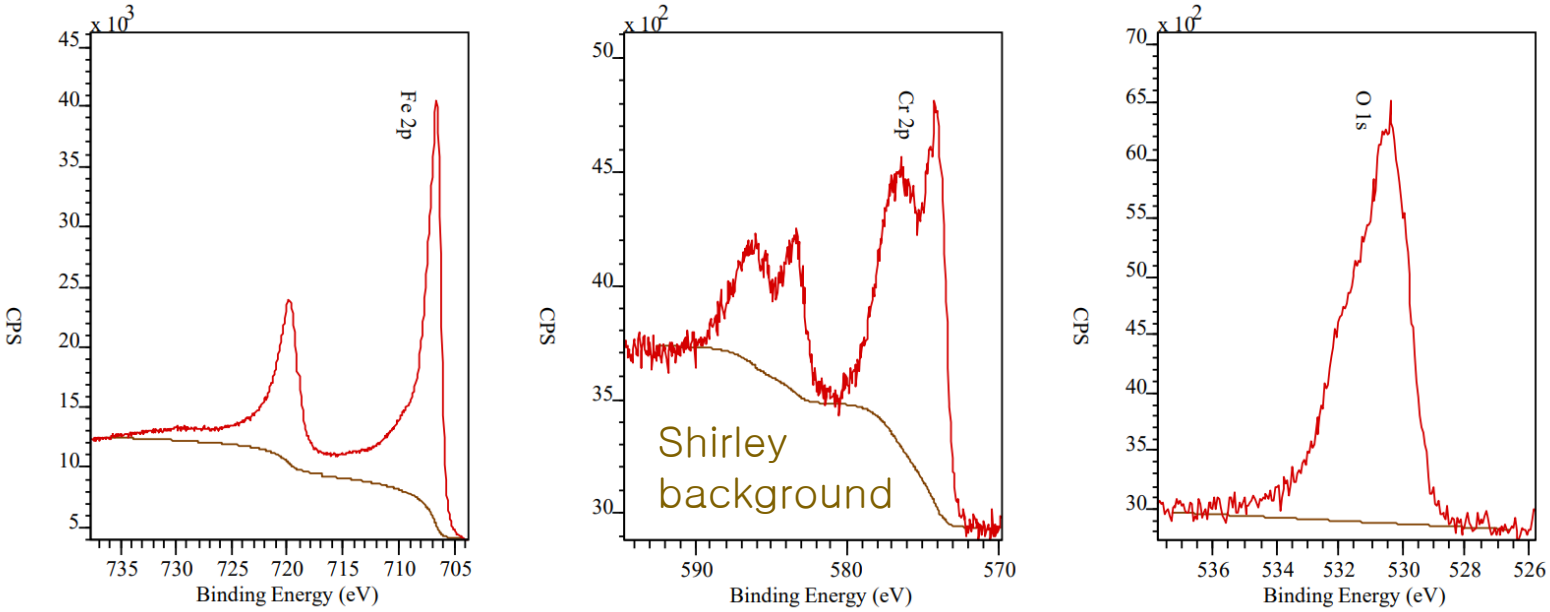

(1) Background subtraction
(2) Area integration
(3) Normalization by sensitivity factor
(4) Atomic percentage

$$Atomic\ \% = \frac{I_A/S_A}{\sum I_i/S_i} \times 100$$

Line	R.S.F.	Line	R.S.F.
Mg KLL (a)	4.300	Ag 3d	5.987
S 2p	0.668	Ag 3d5/2	3.592
S 2p3/2	0.445	Cd 3d	6.623
K 2p	1.466	Cd 3d5/2	3.974
K 2p3/2	0.977	In 3d	7.265
Ca 2p	1.833	In 3d5/2	4.359
Ca 2p3/2	1.222	Sn 3d	7.875
Ti 2p	2.001	Sn 3d5/2	4.725
Ti 2p3/2	1.334	Sn 3p	2.254
V 2p	2.116	Sn 3p3/2	1.503
V 2p3/2	1.411	Sb 3d	8.627
Cr 2p	2.427	Sb 3d5/2	5.176
Cr 2p3/2	1.618	Sb 3d3/2	3.451
Mn 2p	2.659	Sb 3p	2.333

http://www.xpsfitting.com/2009/04/relative-sensitivity-factors-rsf.html (22.09.16)

Example

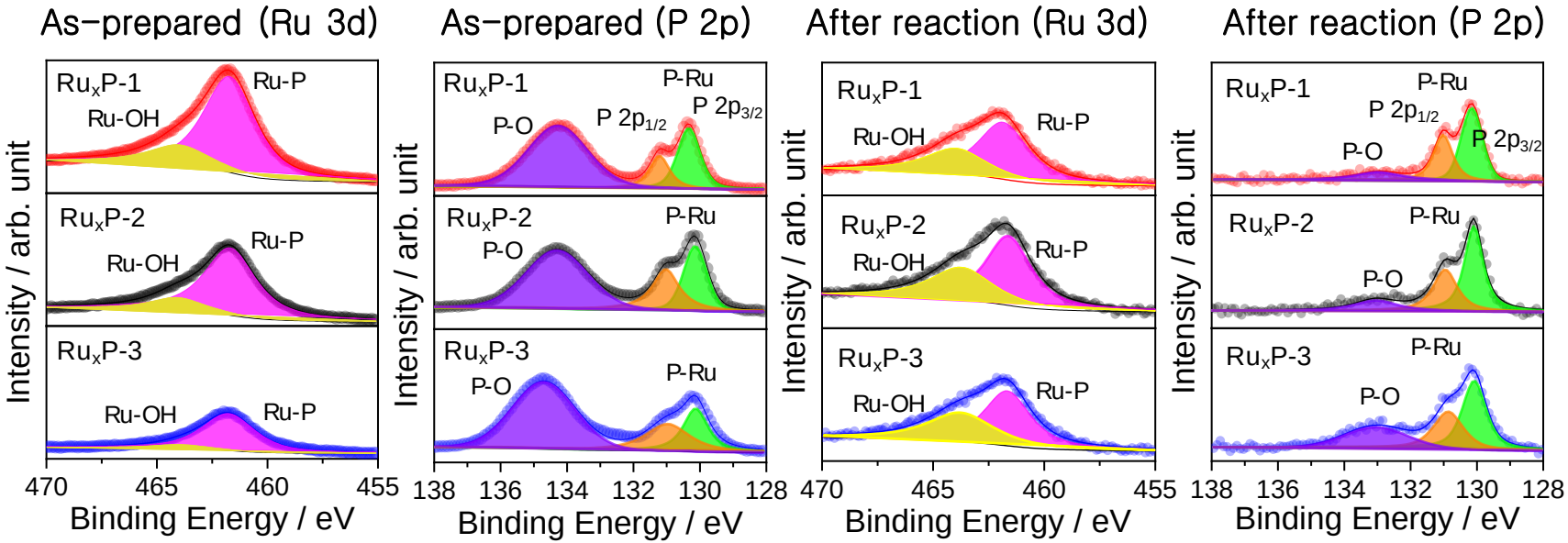

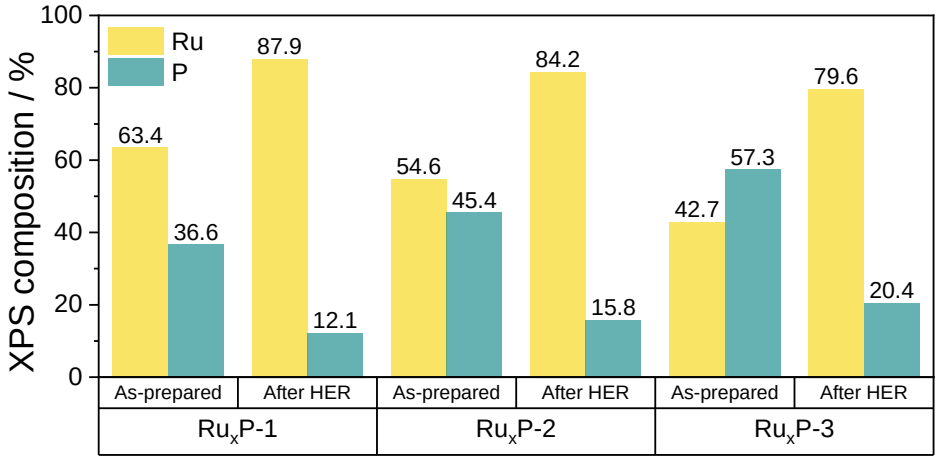

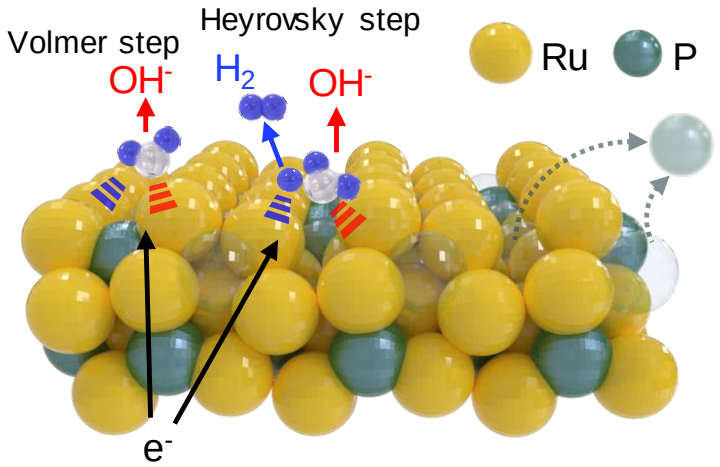

After H_2 evolution reaction, (1) Ru/P ratio increases at the surface
(2) Ru-OH/Ru-P ratio increases while (3) P-O/P-Ru ratio decreases
→ **Exposure of Ru-rich surface** → Ru-rich surface is more catalytically active

https://doi.org/10.1039/C9TA13476J (22.09.16)

Angle-resolved depth profiling

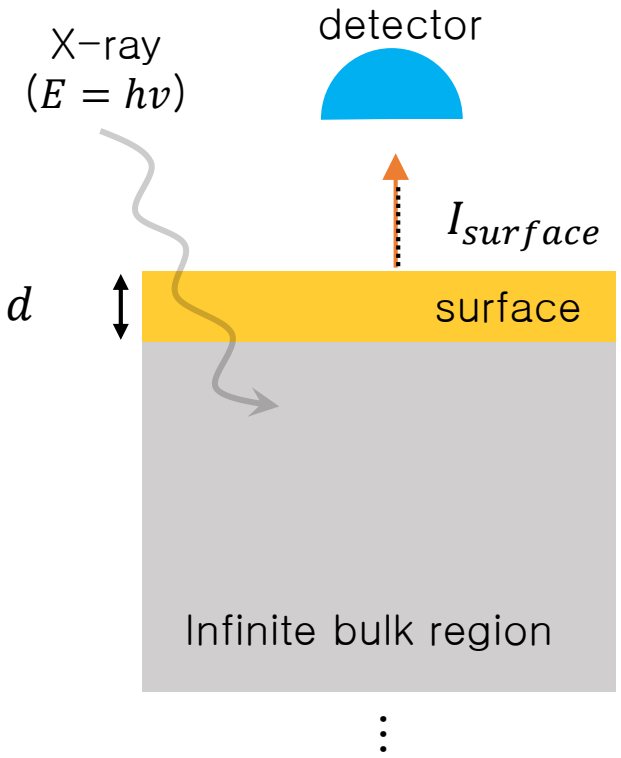

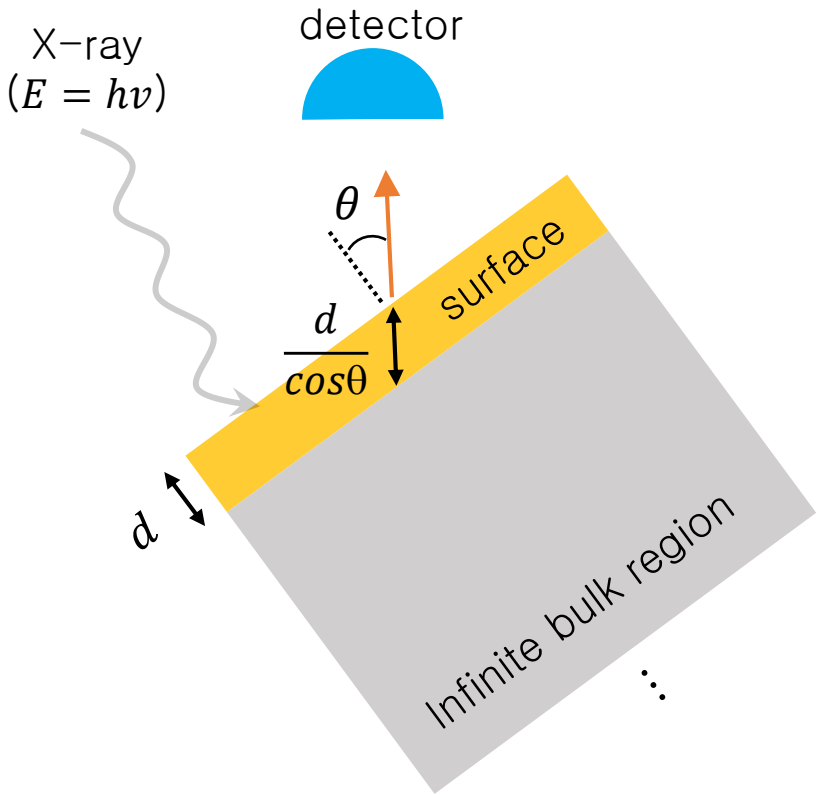

$$I_{surface} = I_{\infty}\left[1 - exp\left(-\frac{d}{\lambda}\right)\right]$$

95.0% from the surface
when d = 3λ

$$I_{surface} = I_{\infty}\left[1 - exp\left(-\frac{d}{\lambda cos\theta}\right)\right]$$

95.0% from the surface
when d = 3λcosθ

Sampling depth decreases with angle !

Angle-resolved depth profiling

- As **sample angle** increases, sampling depth decreases

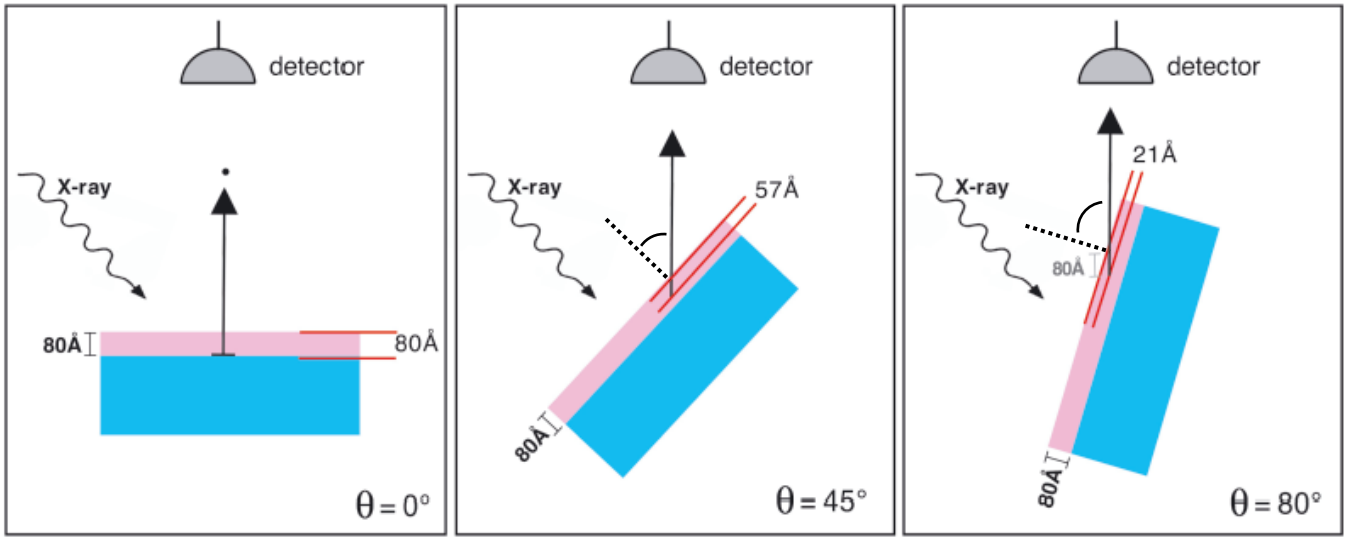

(ex) metal film

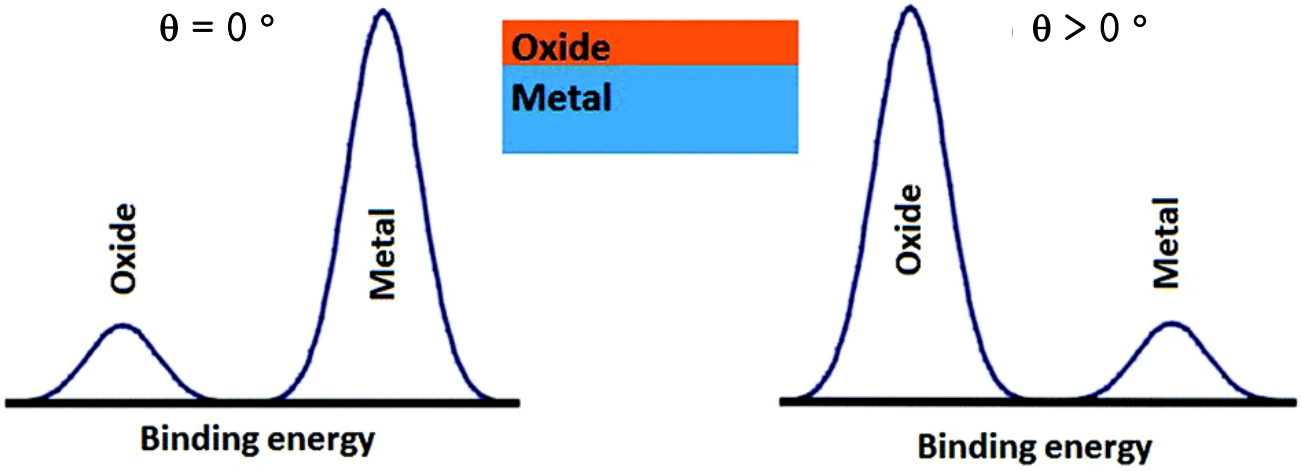

https://doi.org/10.1039/C5RA14139G (22.09.16)

J. C. Vickerman, Surface Analysis-The principal Techniques, 2nd Ed., John Wiley & Sons, Ltd., 2009, p. 91

Energy-resolved depth profiling

- Depth profiling can also be performed using X-ray sources of different energies.
- higher energy X-ray source → higher KE photoelectrons → increased sampling depth

(ex) If Al Kα (1487 eV), Ag Lα (2984 eV), and Cr Kα (5415 eV) X-ray sources are each used, the C 1s electron sampling depths can be estimated at 10.8, 16.2, and 22.4 nm, respectively.

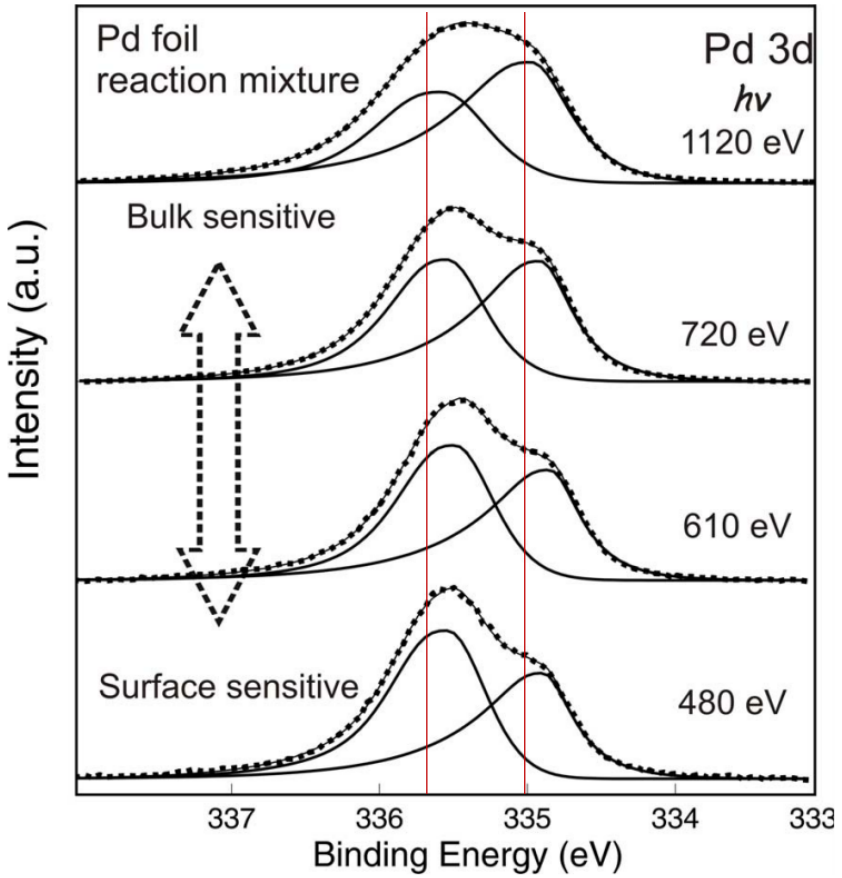

Not only adsorbate-induced surface core level shift !

But on-top location!

https://doi.org/10.1016/j.jcat.2006.05.030 (22.09.16)

Destructive depth profiling

– Ion etching → analysis → ion etching → analysis …

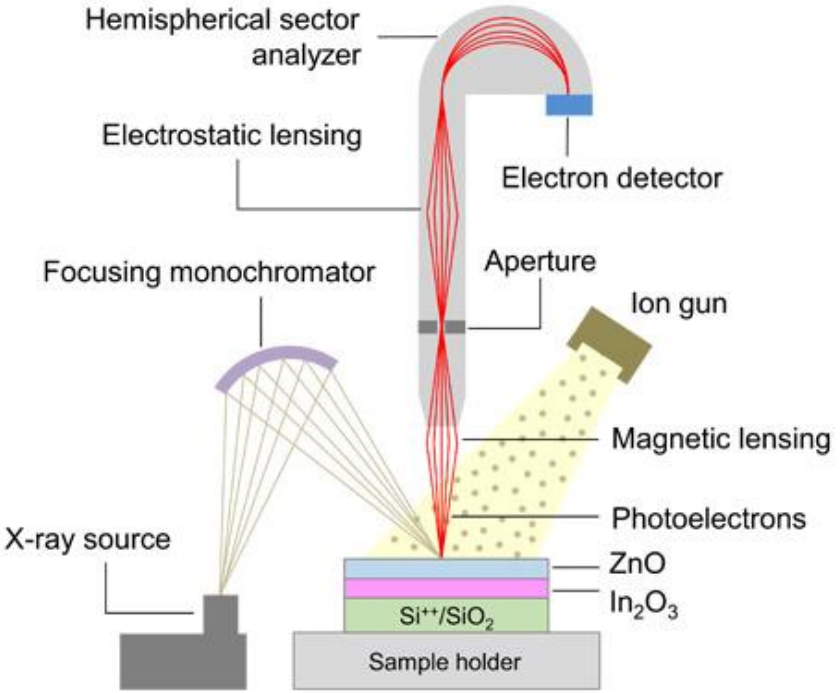

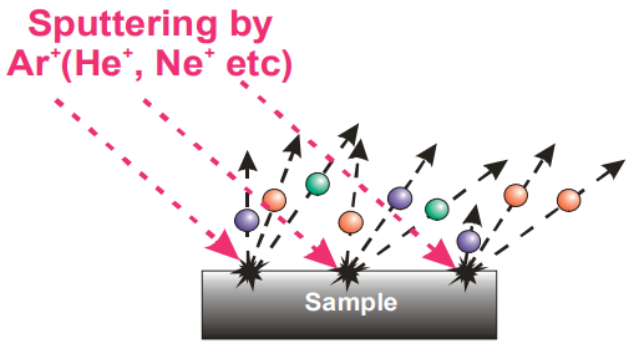

Sci. Adv. **2017**, *3*, e1602640

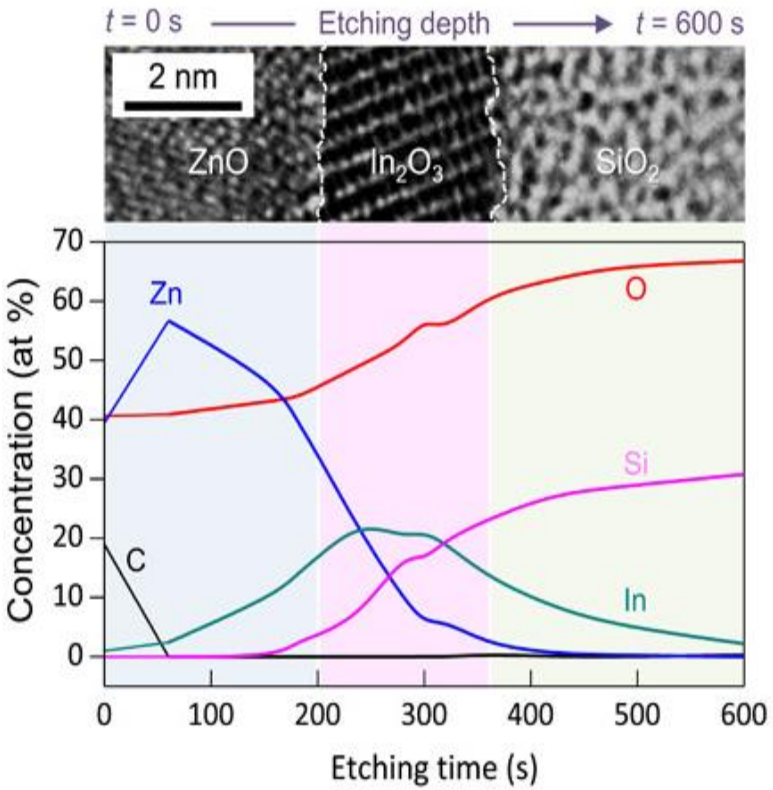

https://doi.org/10.1126/sciadv.1602640 (22.09.16)

Mapping and imaging

- microprobe mode where the X-rays are focused to a small spot on the sample can be utilized for improving the spatial resolution (~5 μm).

- Spatial resolutions of XPS are poorer than those of other surface analysis techniques such as AES and SIMS. It is hard to focus an X-ray beam than an electron or ion beam.

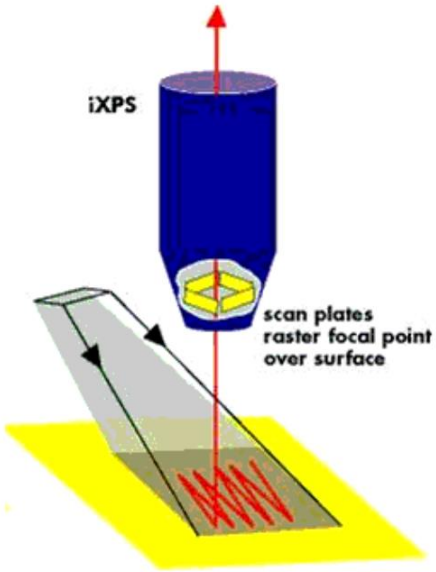

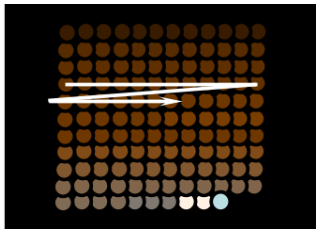

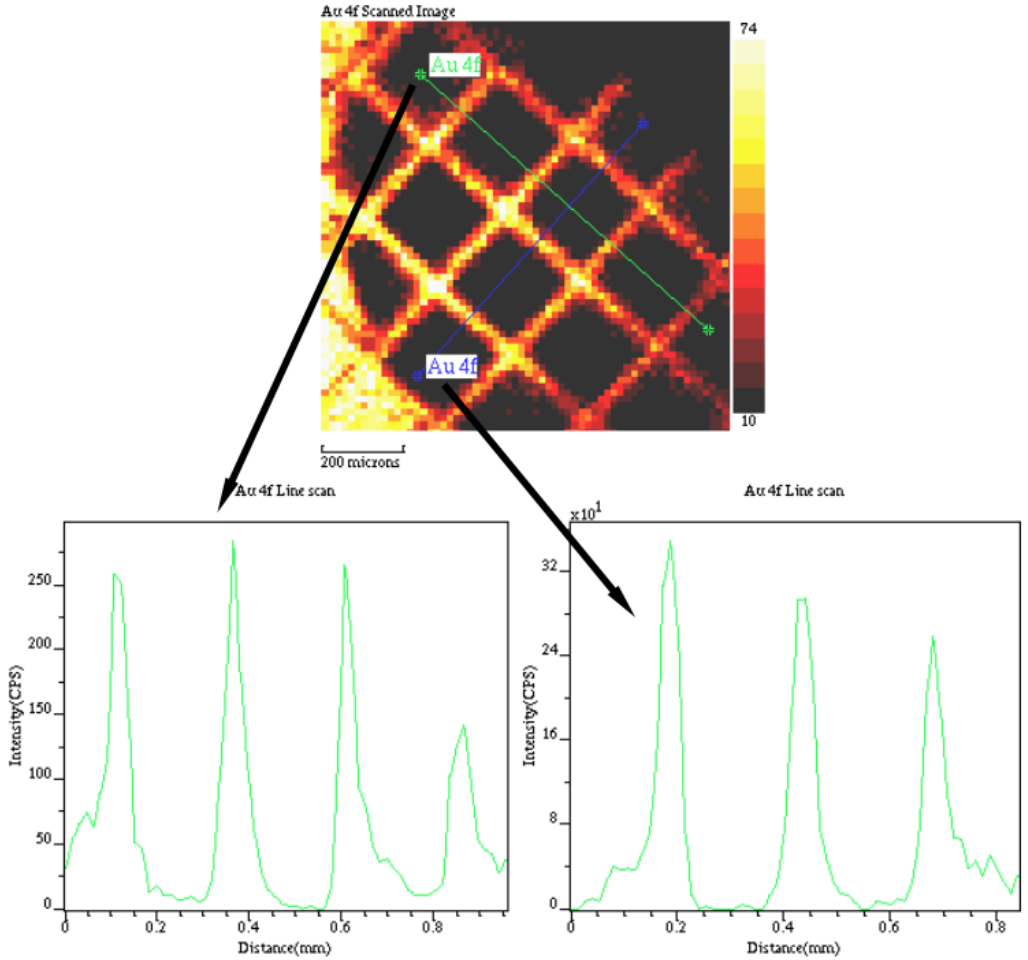

In situ XPS

Conventionally, UHV condition is required to avoid electron scattering with gas molecules → Differential pumping & advanced collecting lens

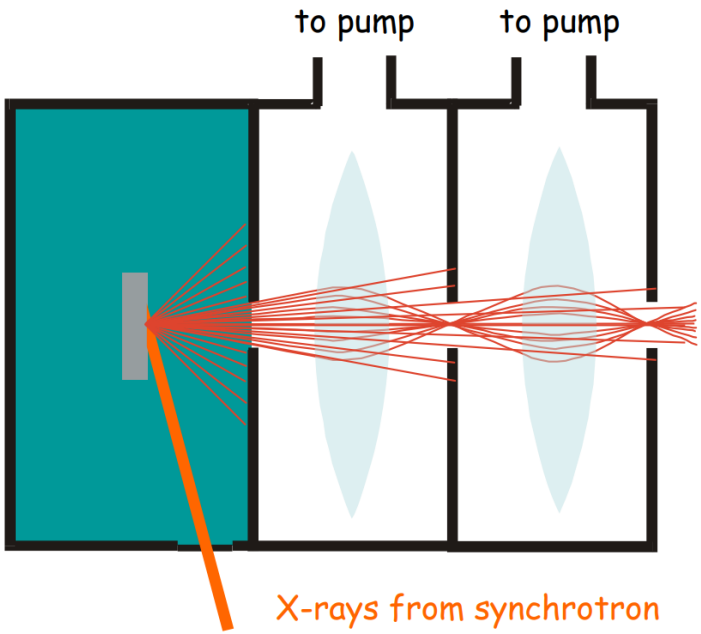

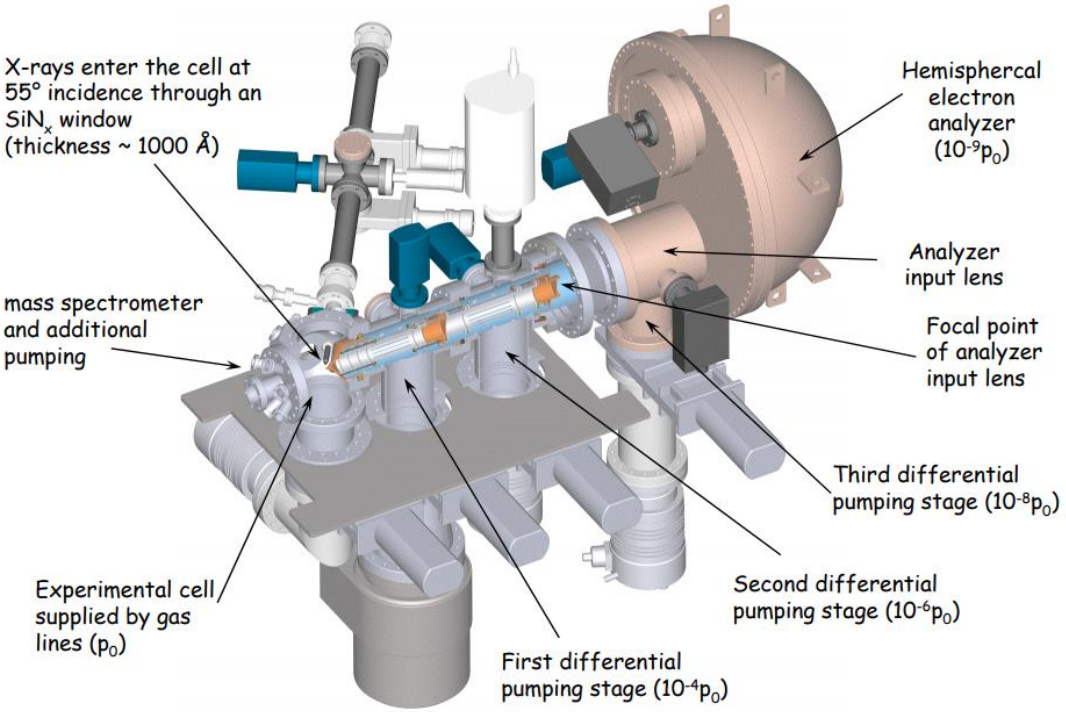

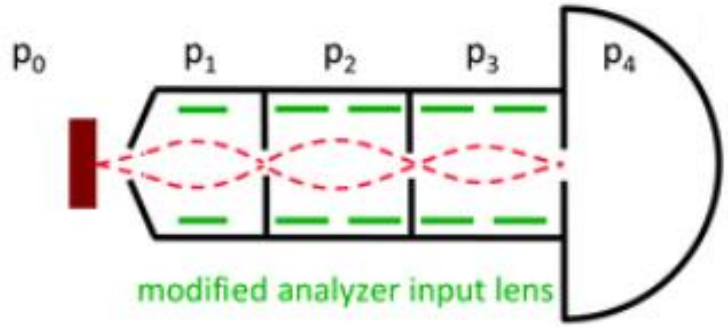

https://webapp.uibk.ac.at/physchem/nmci/research/topics/interfacial-engineering (22.09.16)

https://doi.org/10.1039/C3CS60057B (22.09.16)

In situ XPS

Observation of solid–liquid interface using "dip & pull" method

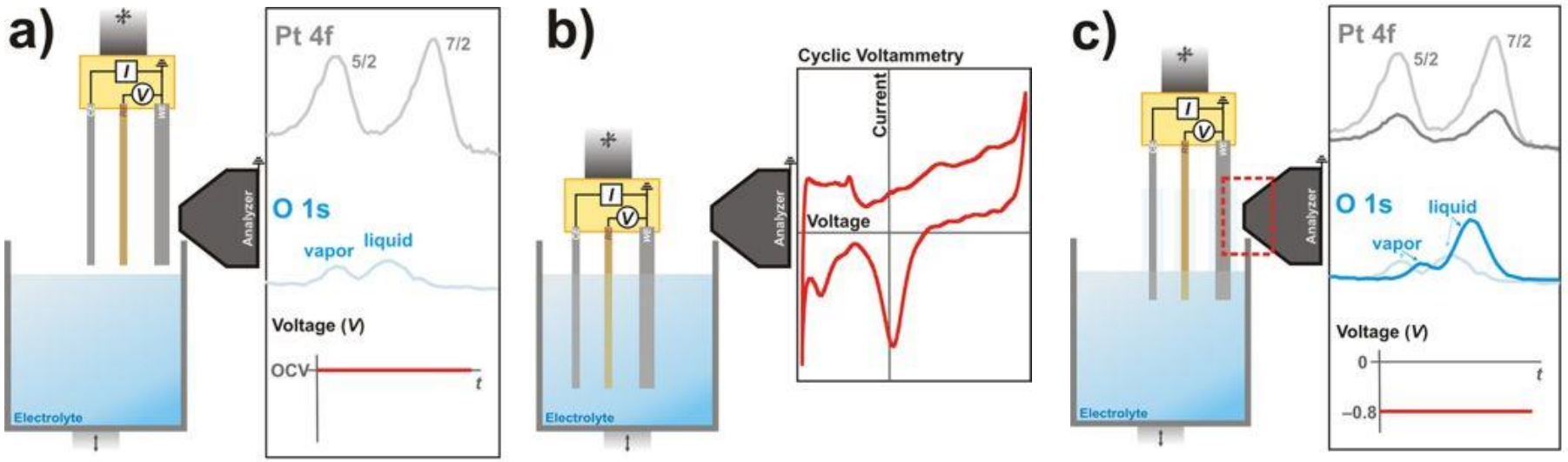

"tender" X-ray (2 keV–7 keV) provides an optimal energy region for photoelectrons to extract information from the interface region

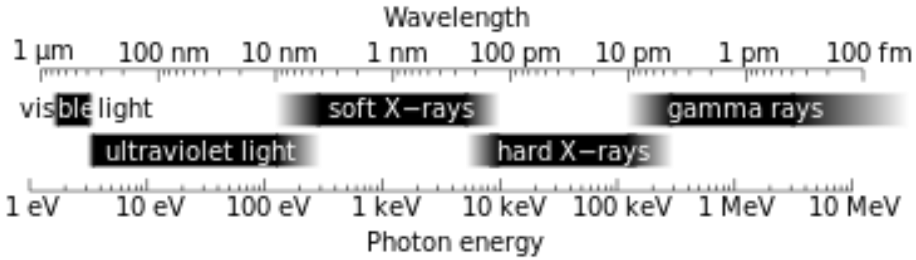

https://en.wikipedia.org/wi

https://en.wikipedia.org/wiki/X-ray (22.09.16)

https://doi.org/10.1038/srep09788 (22.09.16)

Surface analysis techniques

Topography: the surface shape and features of an area
SEM (scanning electron microscopy), STM (Scanning tunneling microscope)
XPS (X-ray photoelectron spectroscopy), ESCA (Electron spectroscopy for chemical analysis)
AES (Auger electron spectroscopy), SIMS (Secondary-ion mass spectrometry)

Table 1.1 Surface analysis techniques and the information they can provide

Radiation IN / Radiation DETECTED	photon / electron	photon / photon	electron / electron	ion / ion	neutron / neutron
SURFACE INFORMATION					
Physical topography			SEM STM (9)		
Chemical composition	ESCA/XPS (3)		AES (2)	SIMS (5) ISS (6)	
Chemical structure	ESCA/XPS (3)	EXAFS (8) IR & SFG (7)	EELS (7)	SIMS (4)	INS (7)
Atomic structure		EXAFS (8)	LEED RHEED (8)	ISS (6)	
Adsorbate bonding		EXAFS (8) IR (7)	EELS (7)	SIMS (4)	INS (7)

Higher lateral resolution

J. C. Vickerman, Surface Analysis-The principal Techniques, 2nd Ed., John Wiley & Sons, Ltd., 2009, p. 4

Electron beam interactions

Responses = characteristic X-rays + backscattered e^- + secondary e^- + Auger e^-

- secondary e^-:
result of interactions btw e^- beam and **bound electrons** in the solid

- backscattered e^-: e^- is **deflected by electrostatic field** of the positive nucleus and eventually exit from the surface

- Auger e^-: e^- emitted by **relaxation process of excited ion**.
The **low-energy Auger e-** is caused by only a few atomic layers due to **short attenuation length**.

high spatial resolution
at nanometer levels

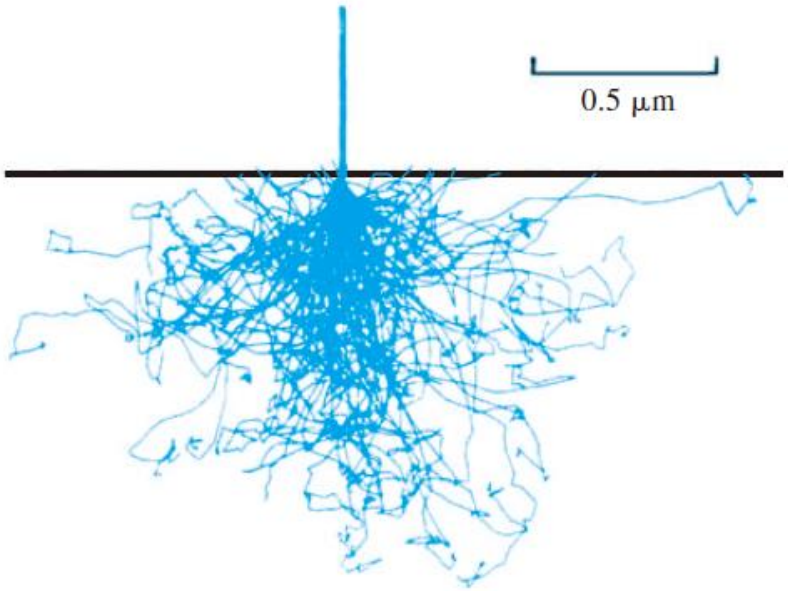

*Simulation of electron trajectories showing the scattering volume of **20-keV electrons** in an iron sample.*

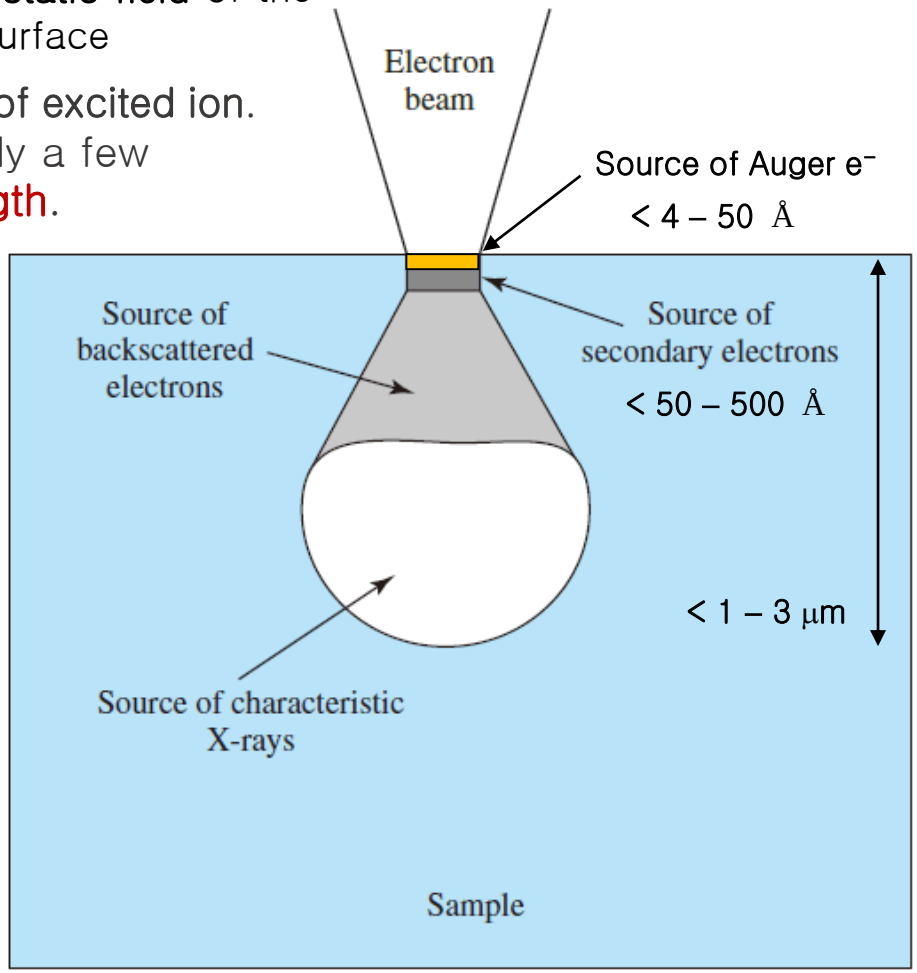

Interaction volumes of various e^- responses

D. A. Skoog, Principles of Instrumental Analysis, 7th Ed., Cengage Learning, 2017, pp. 556-557

Auger Electron Spectroscopy (AES)

Formation process of Auger e^-:

(1) By exposing the analyte to a beam of electrons, the **excitation process** occur

Incident e^- with energy loss

$$A + e_i^- \rightarrow A^{+*} + e_i'^- + e_A^-$$

Incident electron

excited ion

e^- ejected from the inner orbital

(2) **relaxation** of the **excited ion A^{+*}**

$$A^{+*} \rightarrow A^{++} + e_A^-$$

excited ion

relaxed ion

Auger e^-

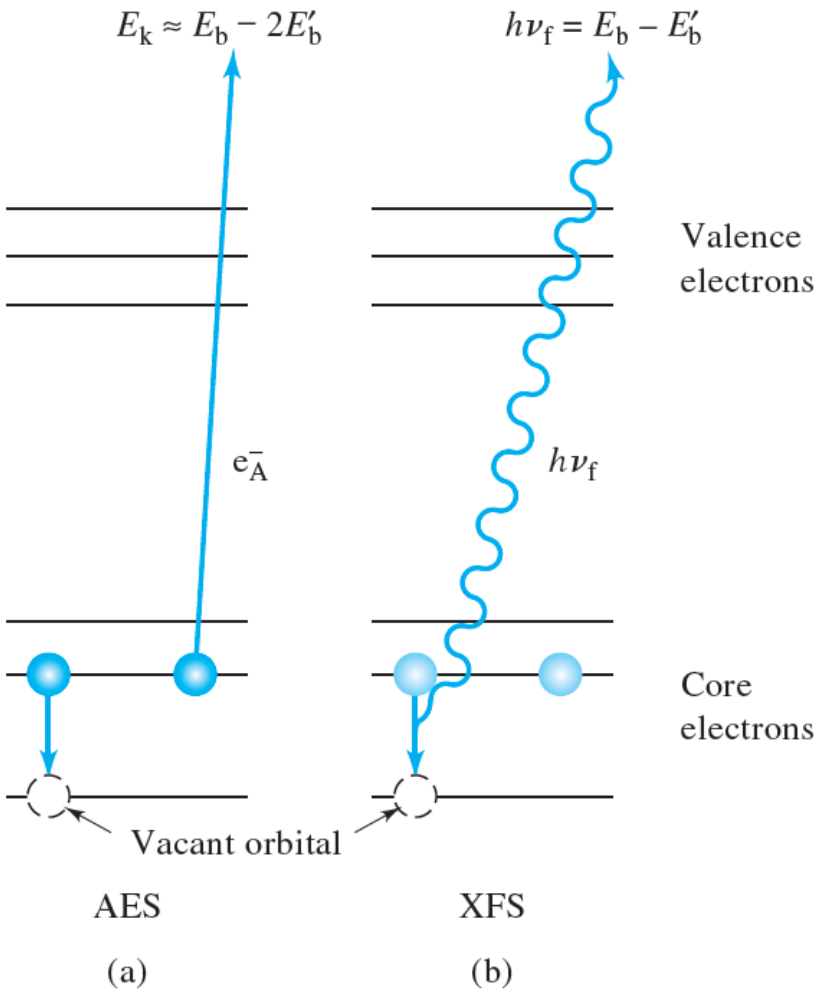

FIGURE 21-7 Schematic representation of the source of (a) Auger electron emission and (b) X-ray fluorescence that competes with Auger emission.

D. A. Skoog, Principles of Instrumental Analysis, 7th Ed., Cengage Learning, 2017, p. 545

Auger Electron Spectroscopy (AES)

the energy released in relaxation of the excited ion

the energy required to remove the second electron from its orbital

$$Auger\ e^- KE = \left(E_K - E_{L_1}\right) - E_{L_1} - \Phi_A$$

$$= \left(E_K(Z) - E_{L_1}(Z+\Delta)\right) - E_{L_1}(Z+\Delta) - \Phi_A$$

Z: atomic number, Φ_A: work function of analyzer

Δ: the displacement of electronic energy level towards higher BE after ionization of the atom by primary electron.

Approximation:

$$E_{L_1}(Z+\Delta) = \frac{1}{2}\left[E_{L_1}(Z) + E_{L_1}(Z+1)\right]$$

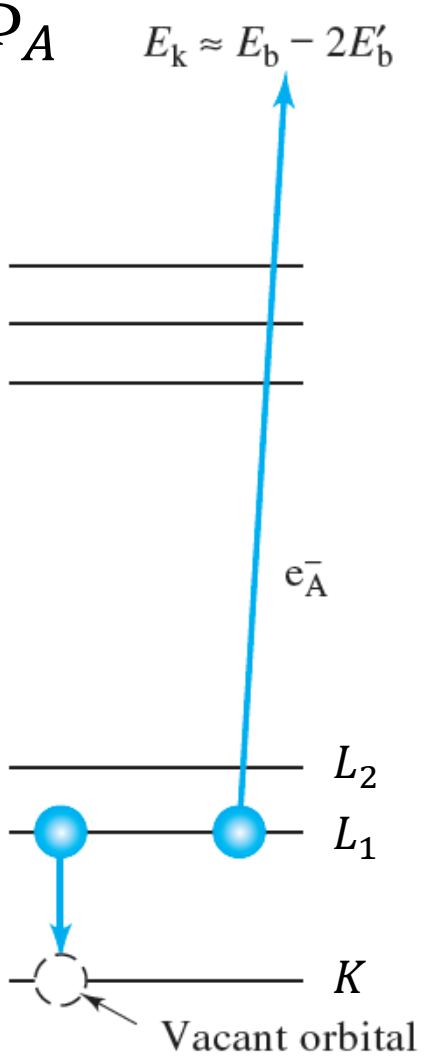

- the KE of Auger e⁻ is **independent of the incident e⁻ energy** that created the vacancy in energy level
- the KE of Auger e⁻ is **involved** with **binding energies** more than one
- In practice, experimental data are used for peak identification

D. A. Skoog, Principles of Instrumental Analysis, 7th Ed., Cengage Learning, 2017, p. 545

Nomenclature for Auger transitions

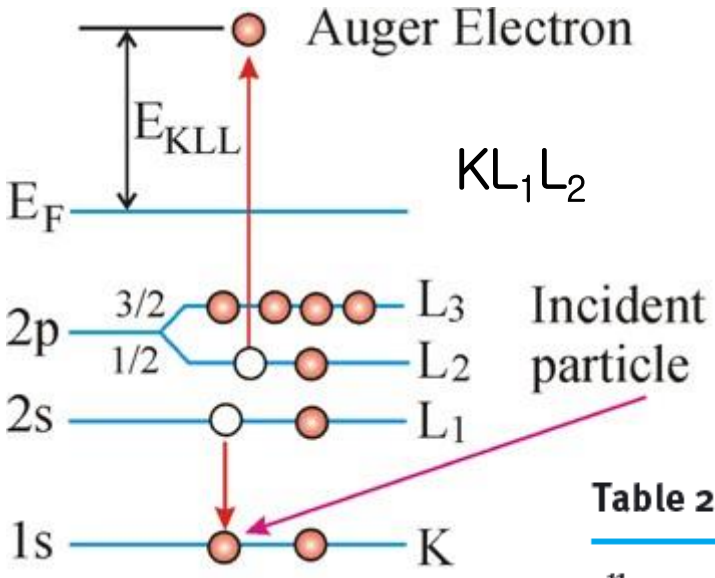

Auger emissions are described in terms of the type of orbital transitions.

For example, **KLL transition** involves:

(1) an initial removal of a **K** e^-
(2) followed by a transition of L_1 e^- to K level
(3) with the ejection of a **second** L_2 e^-.

Table 2.1 Nomenclature of AES and XPS peaks

n	*l*	*j*	Index	AES notation	XPS notation
1	0	1/2	1	K	$1s_{1/2}$
2	0	1/2	1	L_1	$2s_{1/2}$
2	1	1/2	2	L_2	$2p_{1/2}$
2	1	3/2	3	L_3	$2p_{3/2}$
3	0	1/2	1	M_1	$3s_{1/2}$
3	1	1/2	2	M_2	$3p_{1/2}$
3	1	3/2	3	M_3	$3p_{3/2}$
3	2	3/2	4	M_4	$3d_{3/2}$
3	2	5/2	5	M_5	$3d_{5/2}$
etc.			etc.	etc.	etc.

A given energy state is characterized by four quantum numbers, i.e. n (principal quantum number), l (orbital), s (spin) and j (spin–orbit coupling with j = l + s).

https://slideplayer.com/slide/5316389 (22.09.16)

J. C. Vickerman, Surface Analysis-The principal Techniques, 2nd Ed., John Wiley & Sons, Ltd., 2009, p. 11

Nomenclature for Auger transitions

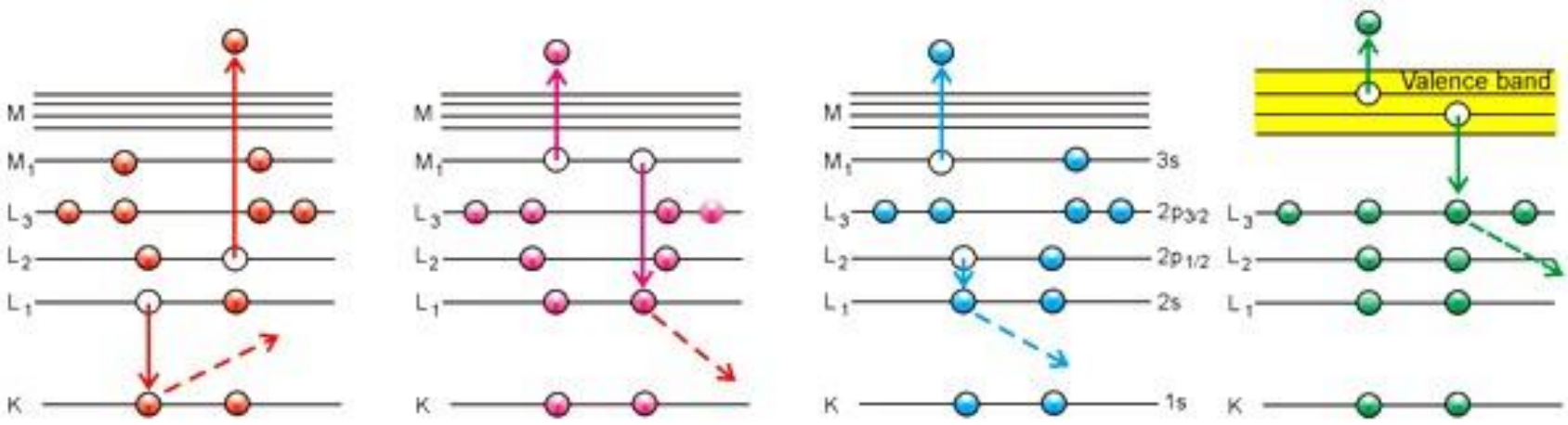

Auger
KL_1L_2

Auger
$L_1M_1M_1$

Coster-Kroning
$L_1L_2M_1$

Auger (Solid)
L_3VV

KL_1L_{23} { KL_1L_1, KL_1L_2, KL_1L_3

e. g. Cu LMM

$L_3M_{23}M_{23}$ (768 eV)
$L_2M_{23}M_{23}$ (775 eV)
$L_3M_{23}M_{45}$ (839 eV)
$L_3M_{23}M_{45}$ (847 eV)
$L_3M_{45}M_{45}$ (919 eV)
$L_2M_{45}M_{45}$ (939 eV)

Also MNN Auger

https://slideplayer.com/slide/5316389 (22.09.16)

Sampling depth

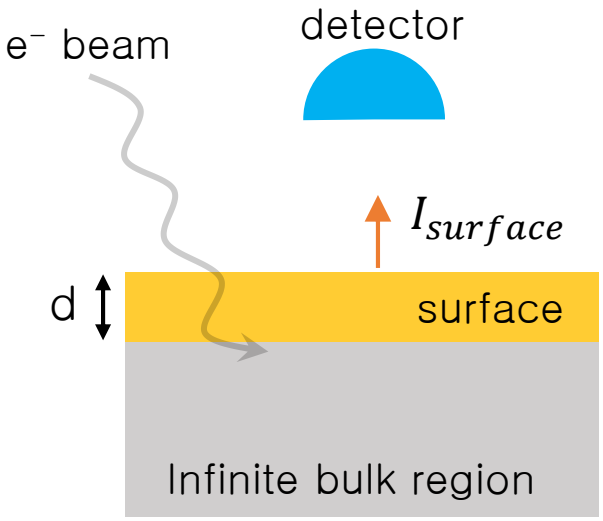

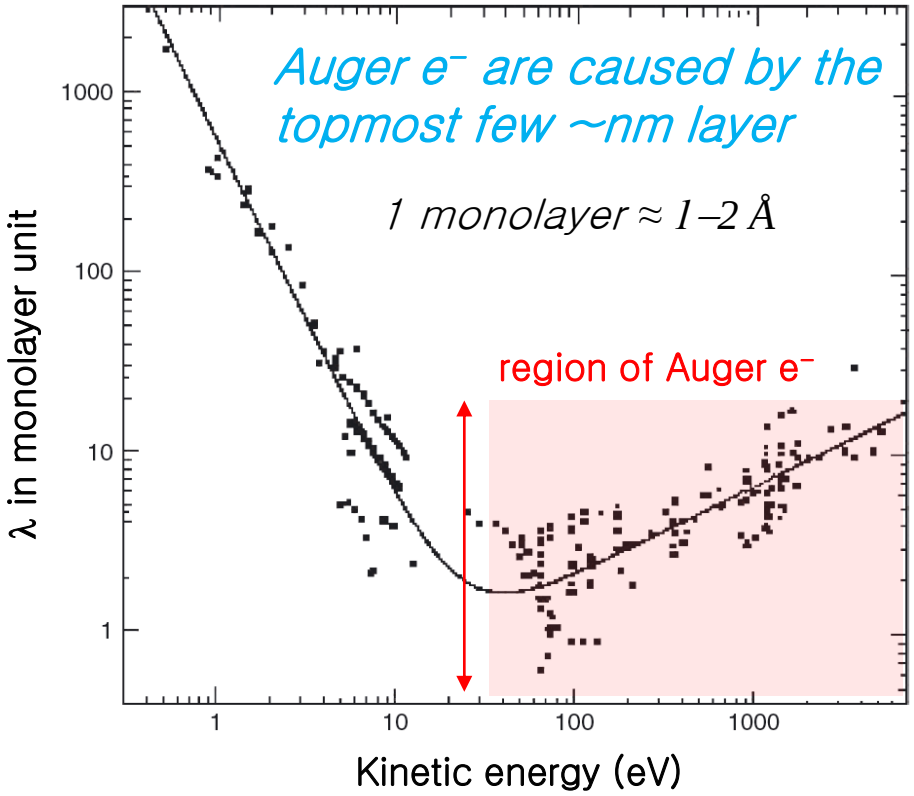

$$I_{surface} = I_{\infty}\left[1 - exp\left(-\frac{d}{\lambda}\right)\right]$$

63.3% from the surface with d = λ
86.4% from the surface with d = 2λ
95.0% from the surface with d = 3λ

Sampling depth

Sampling depth depends on λ

λ depends on KE

$$\text{IMFP} = \lambda = 538\text{KE}^{-2} + 0.41(a\text{KE})^{0.5} \quad \text{(for elements)}$$
$$\text{IMFP} = \lambda = 2170\text{KE}^{-2} + 0.72(a\text{KE})^{0.5} \quad \text{(for inorganic compounds)}$$
$$\text{IMFP} = \lambda_d = 49\text{KE}^{-2} + 0.11\text{KE}^{0.5} \quad \text{(for organic compounds)}$$

J. C. Vickerman, Surface Analysis-The principal Techniques, 2nd Ed., John Wiley & Sons, Ltd., 2009, p. 19

Instrumentation

- AES is similar to XPS in instrumentation except for electron gun
- The cathodic filament, a **W filament being heated**, is maintained **at a potential** of 1 to 50 kV **with respect to the anode**
- Wehnelt cylinder is biased negatively with respect to the filament, which causes the emitted electrons to converge on a tiny spot.
- For W filament, a minimum beam diameter is 3–5 μm
- LaB_6 cathodes and **field emission gun (FEG)** provide much smaller **beam diameter** at **nanometer levels**.

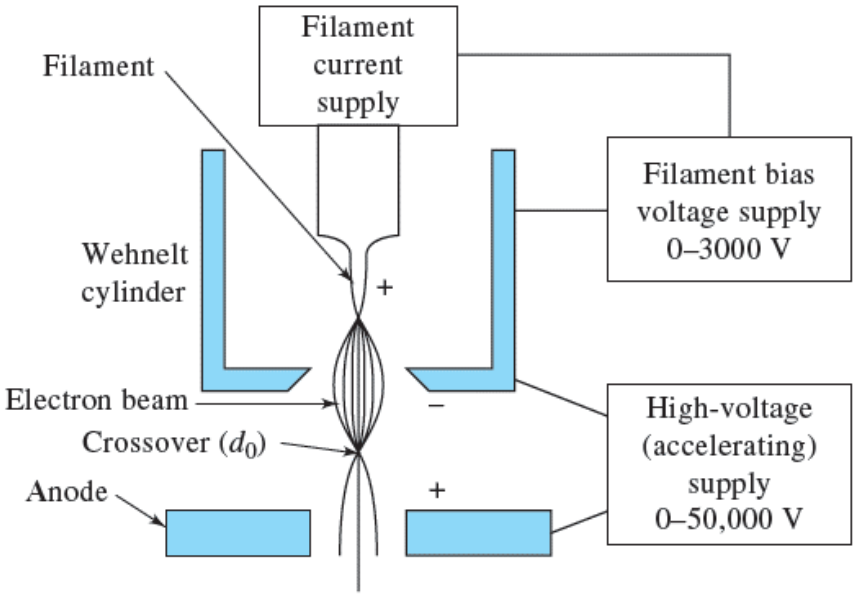

FIGURE 21-9 Block diagram of a tungsten filament source.

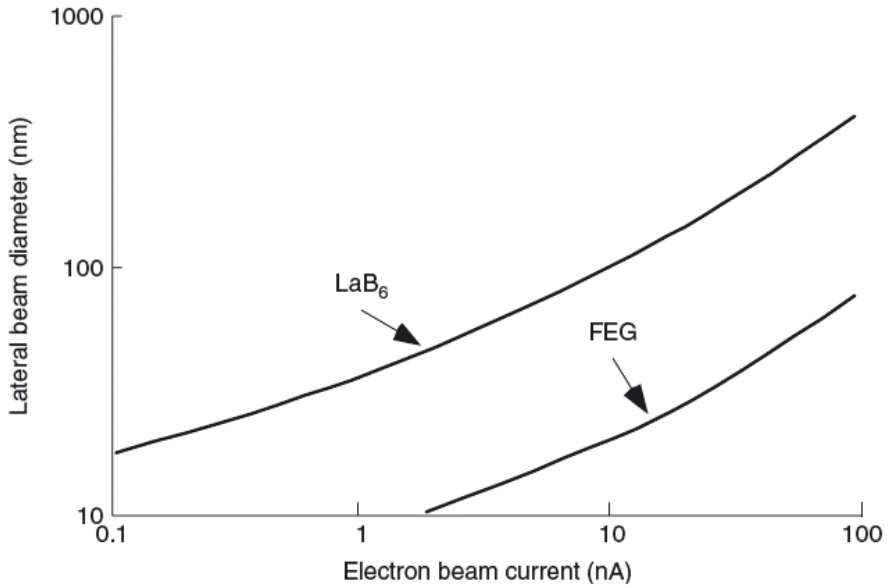

D. A. Skoog, Principles of Instrumental Analysis, 7th Ed., Cengage Learning, 2017, p. 547

J. C. Vickerman, Surface Analysis-The principal Techniques, 2nd Ed., John Wiley & Sons, Ltd., 2009, p. 23

Derivative spectra

– Derivative spectra are standard for Auger spectroscopy to enhance the small peaks and to remove the slowly changing electron backgrounds.

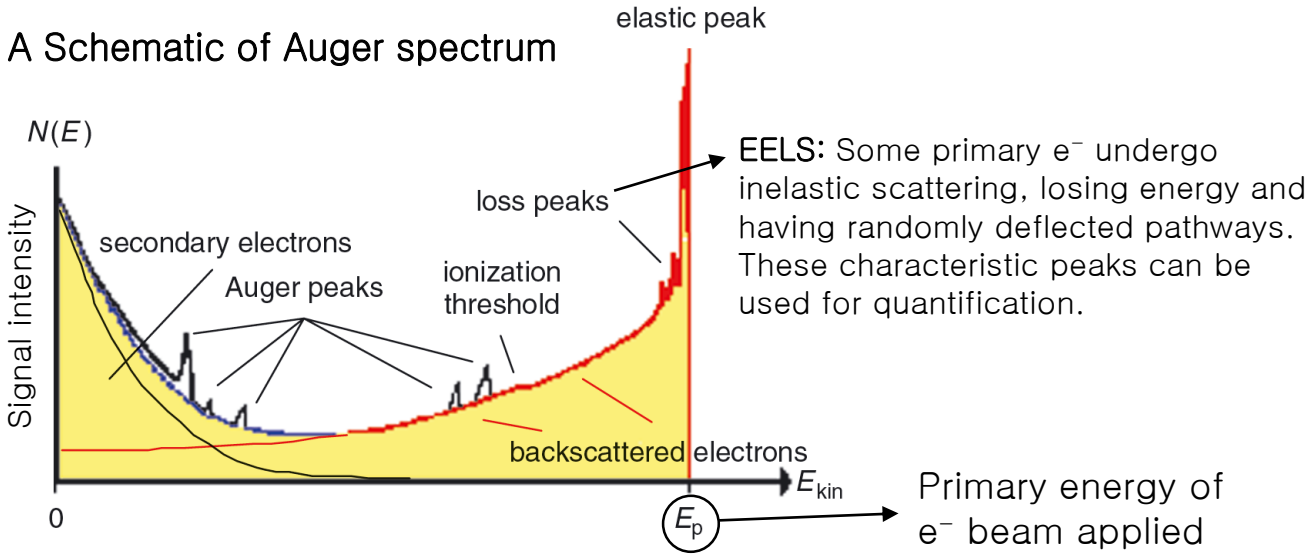

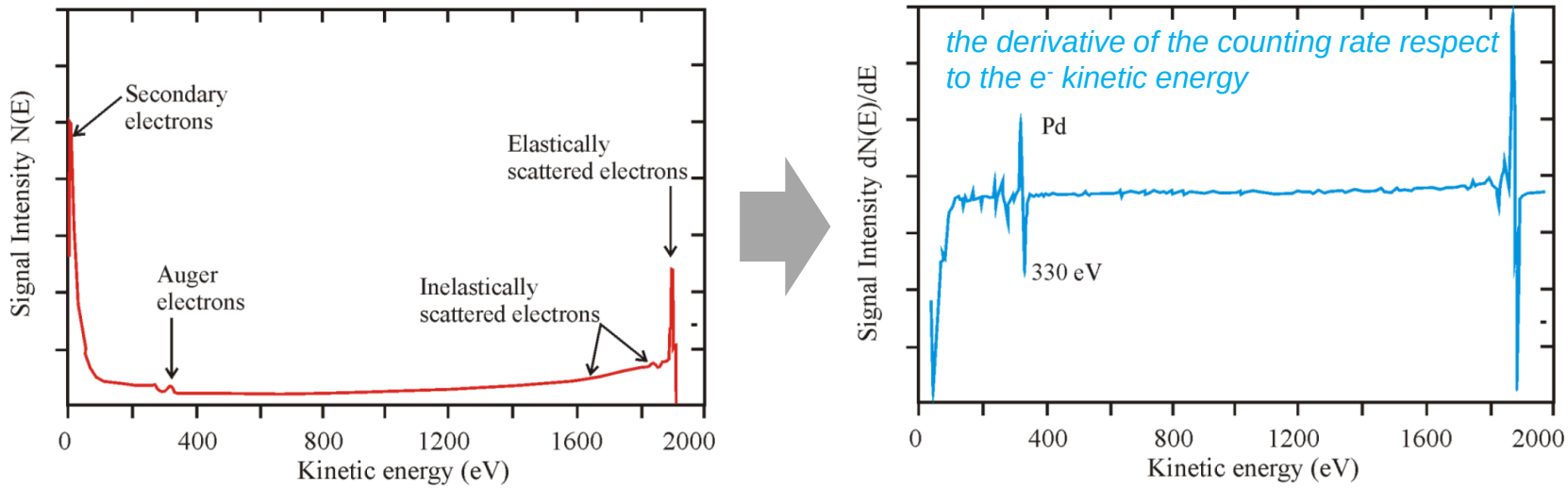

J. C. Vickerman, Surface Analysis-The principal Techniques, 2nd Ed., John Wiley & Sons, Ltd., 2009, p. 12

Qualitative identification of elements

- **Different elements** show **different KEs** for Auger transitions.
- Identification of elements !

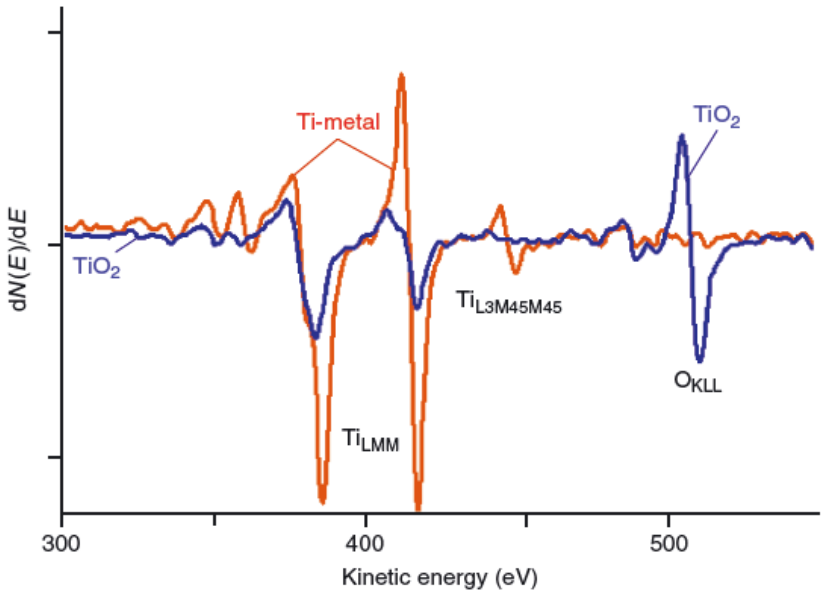

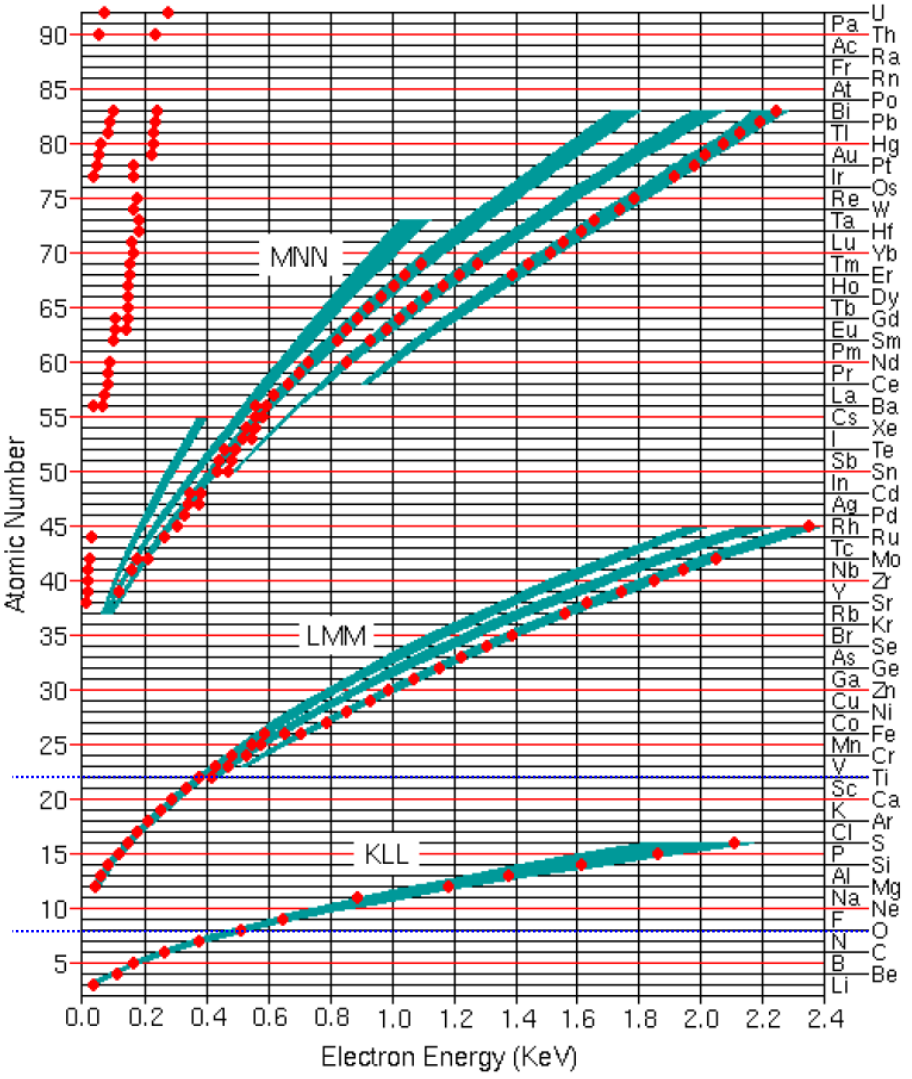

https://www.eag.com/resources/tutorials/auger-tutorial-theory/ (22.09.16)

J. C. Vickerman, Surface Analysis-The principal Techniques, 2nd Ed., John Wiley & Sons, Ltd., 2009, p. 20

Qualitative identification of elements

(1) Comparing the positions of major peaks with Auger energy table
(2) Referring to standard spectra for confirmation
(3) Labelling peaks → Fe, Cr and Ni are identified

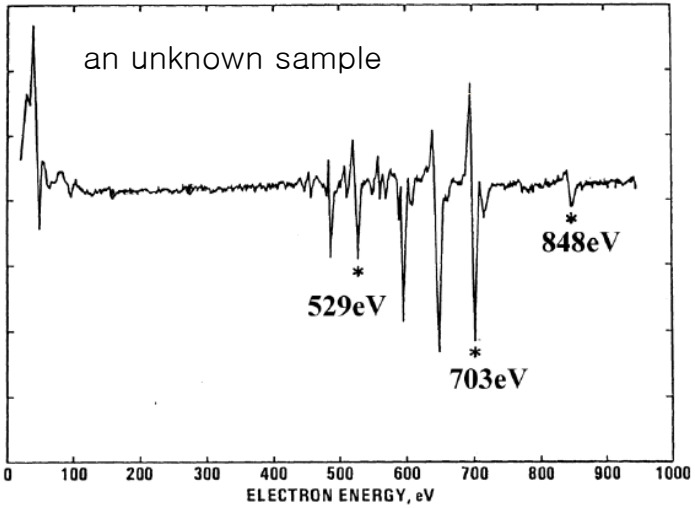

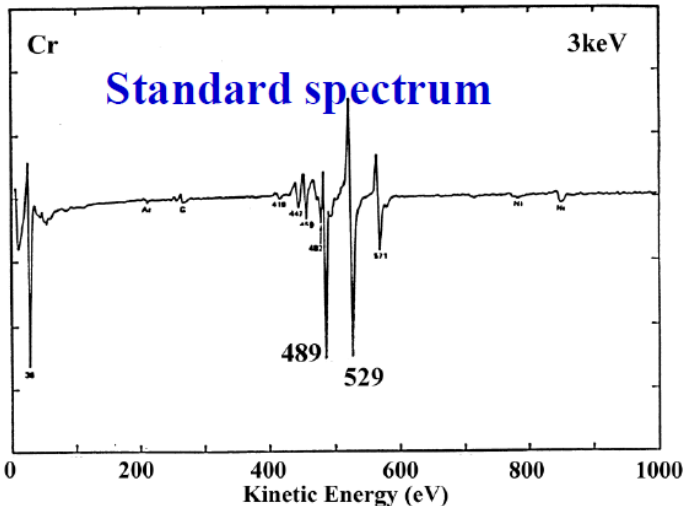

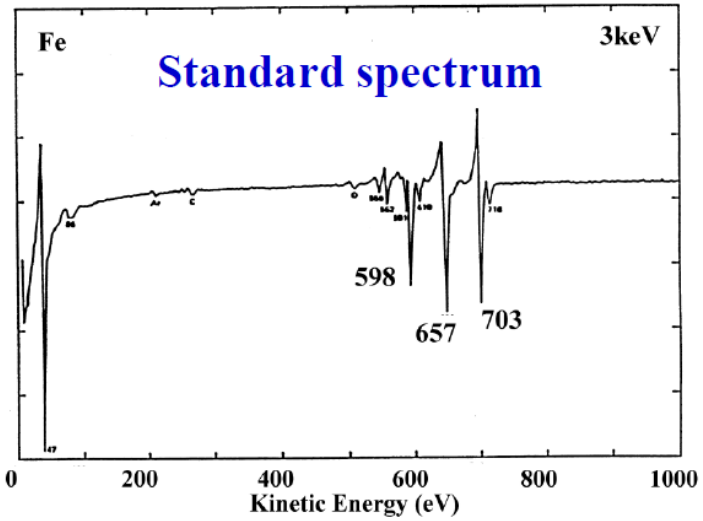

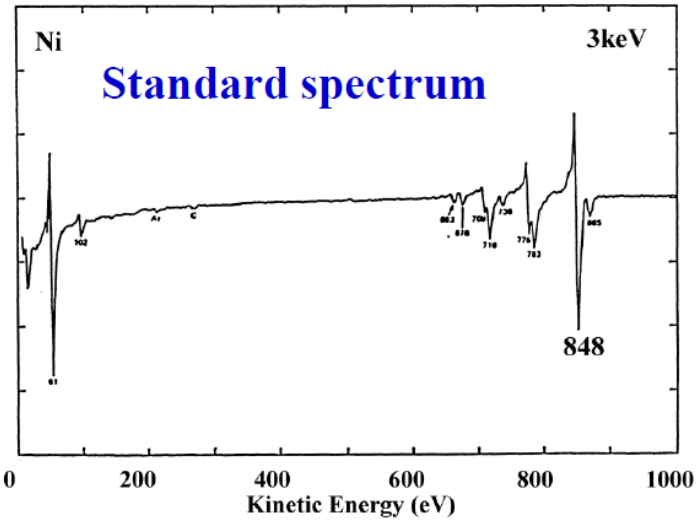

https://slideplayer.com/slide/5316389/ (22.09.16)

Quantitative analysis

$$atomic\ \% = \frac{I_A/S_A}{\sum I_i/S_i} \times 100$$

I_i = the peak-to-peak intensities of the elemental peaks
S_i = the relative sensitivity factor

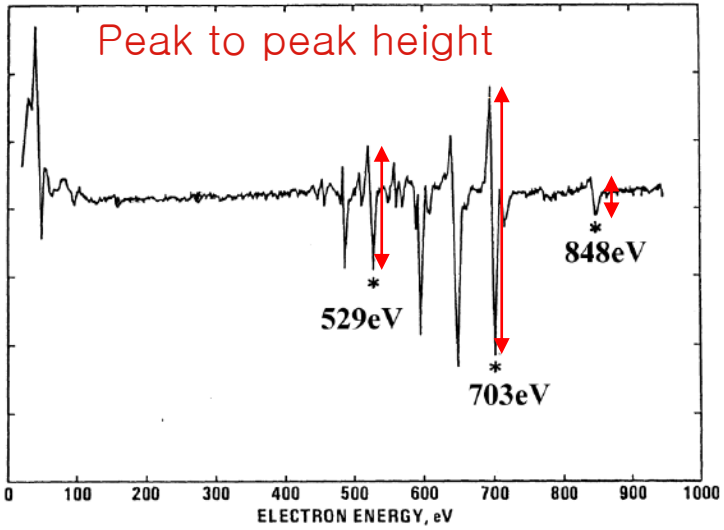

Peak	I_i	S_i
Cr at 529 eV	4.7	0.32
Fe at 703 eV	10.1	0.20
Ni at 848 eV	1.5	0.27

$$\text{Cr}\ \% = \frac{4.7/0.32}{4.7/0.32 + 10.1/0.20 + 1.5/0.27} \times 100 = 21\%$$

https://slideplayer.com/slide/5316389/ (22.09.16)

Relative sensitivity factors

Since for an Auger transition a minimum of three electrons is required, only elements with $Z \geq 3$ can be analyzed.

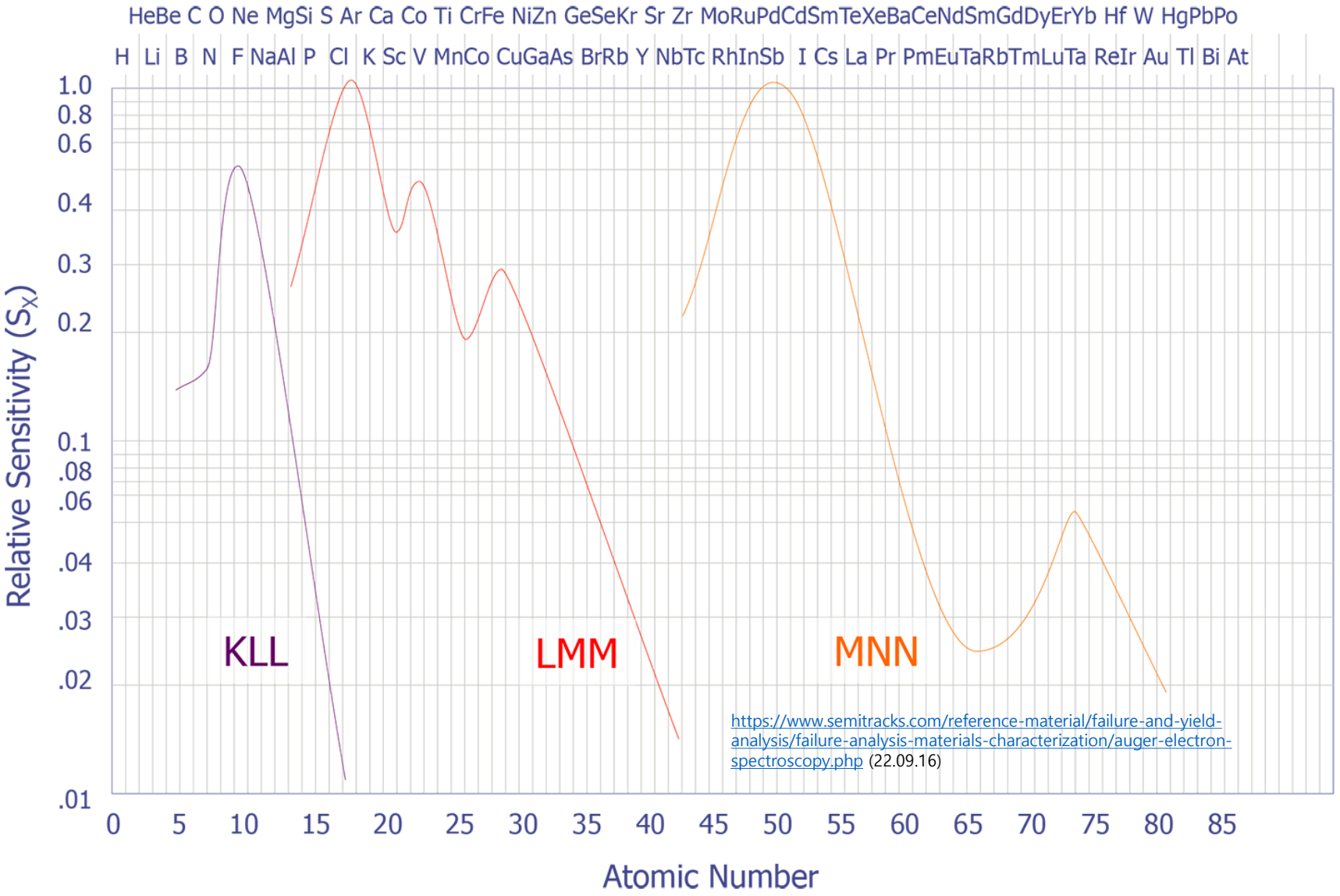

Chemical shift

- A change in the oxidation state → BE change → KE shift
- However, since three energy levels are involved in an Auger transition, the chemical shift cannot be simply correlated with oxidation state.

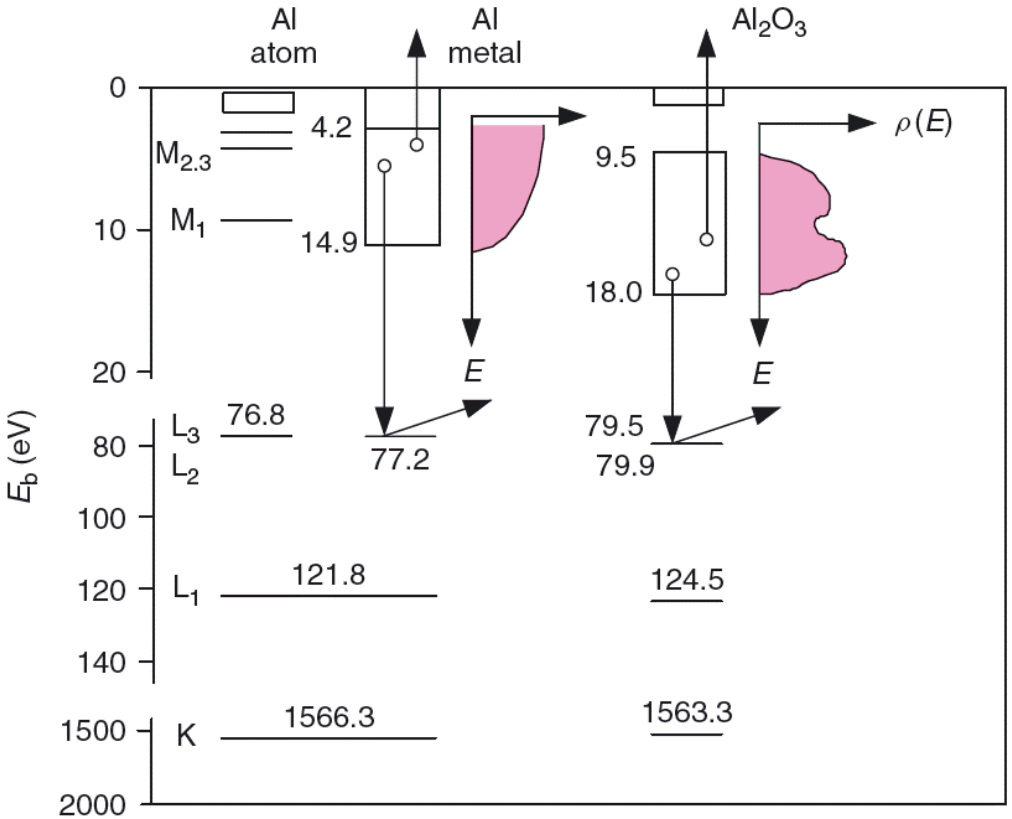

Energy levels of Al atom, Al metal and Al_2O_3

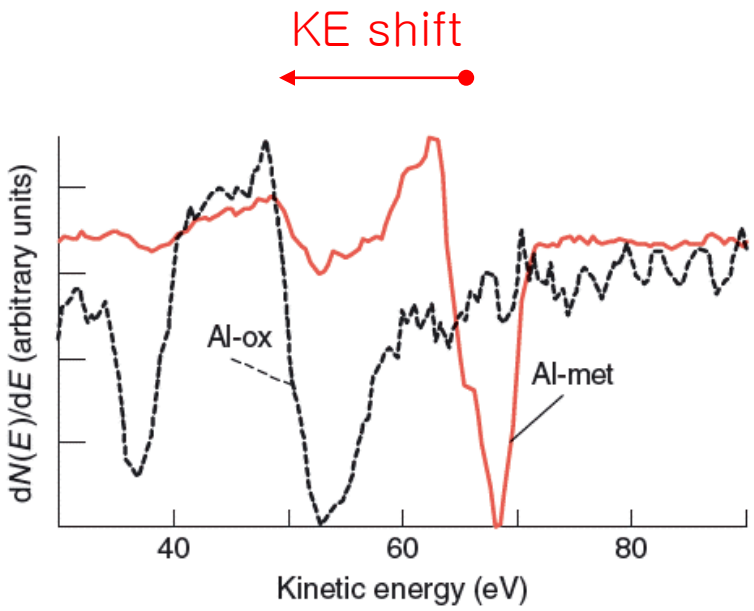

Auger Al_{LMM} peaks of Al metal and Al_2O_3

J. C. Vickerman, Surface Analysis-The principal Techniques, 2nd Ed., John Wiley & Sons, Ltd., 2009, p. 20, p. 43

Example

- **Corrosion resistance** of Cu–Ni alloy is enhanced by anodic oxidation.
- AES spectra reveal the chemical differences between two samples.

- In oxidized sample, **Cu/Ni ratio** decrease Furthermore, the **O/Ni ratio** increases.

→ The corrosion resistance *results from the formation of a* ***nickel oxide surface.***

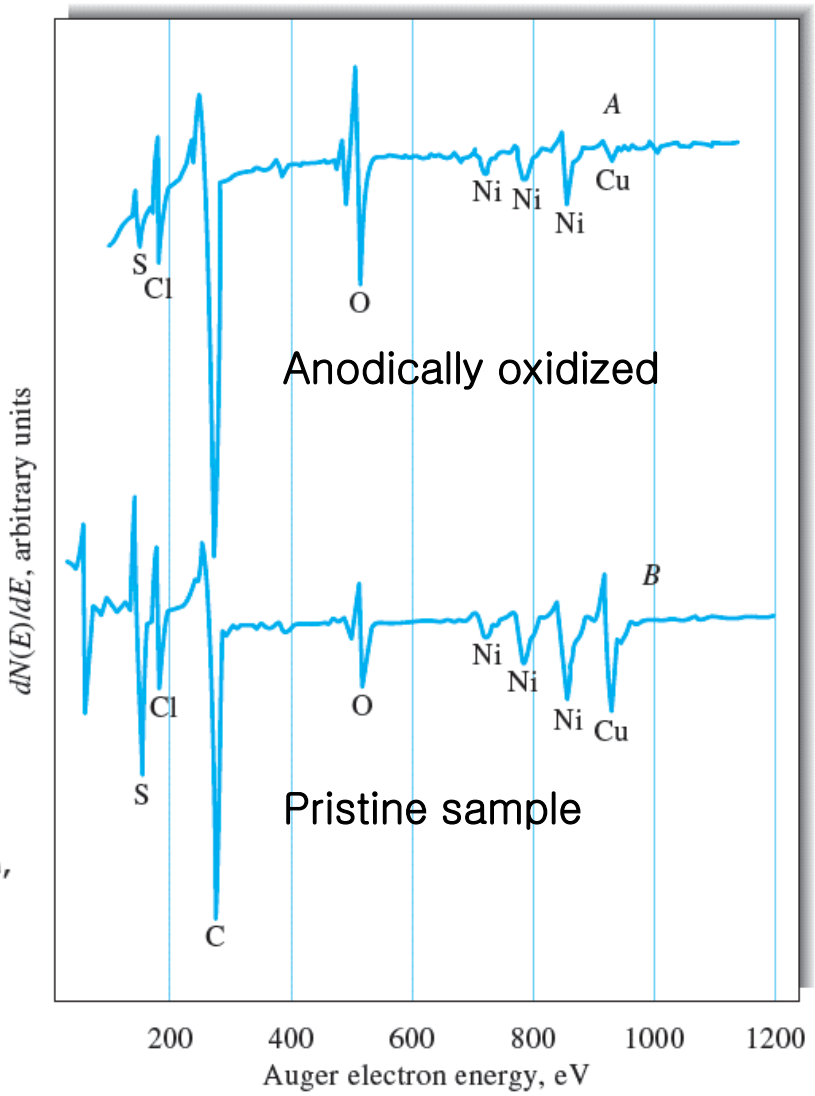

FIGURE 21-8 Auger electron spectra for a 70% Cu:30% Ni alloy. *A*, passivated by anodic oxidation; *B*, not passivated. (Adapted from G. E. McGuire et al., *J. Electrochem. Soc.*, **1978**, *125*, 1801, **DOI:** 10.1149/1.2131298. Reprinted by permission of the publisher, the Electrochemical Society, Inc.)

D. A. Skoog, Principles of Instrumental Analysis, 7th Ed., Cengage Learning, 2017, p. 546

Various acquisition mode

Acquisition modes: (1) point analysis, (2) Line scan, (3) Mapping, (4) Angle-resolved and destructive depth profiling

The line-scan profile

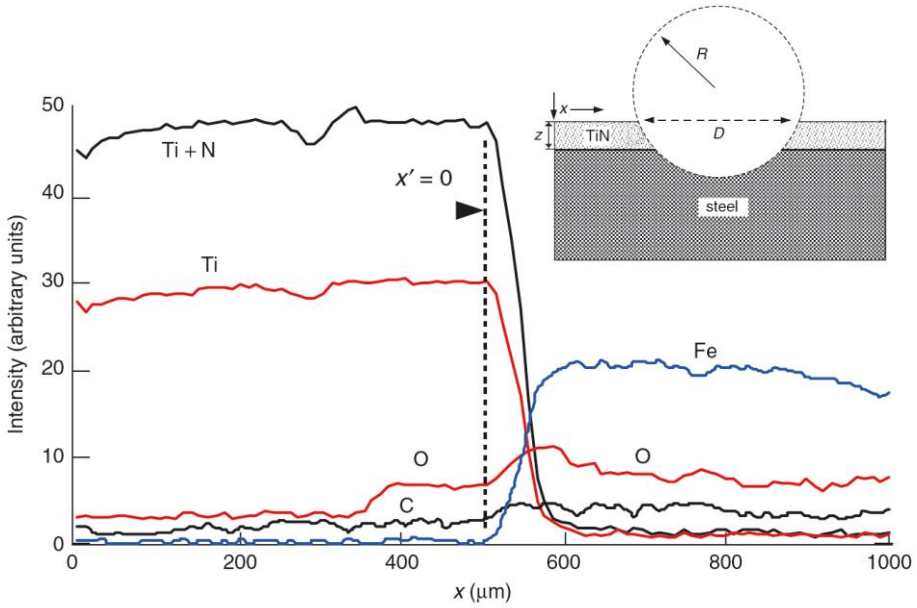

Figure 2.18 Example of a line scan over the crater edge produced by ball cratering showing the atomic concentration as a function of the displacement of the electron beam. The crater edge is located at approximately $x = 500$ μm

Elemental mapping images

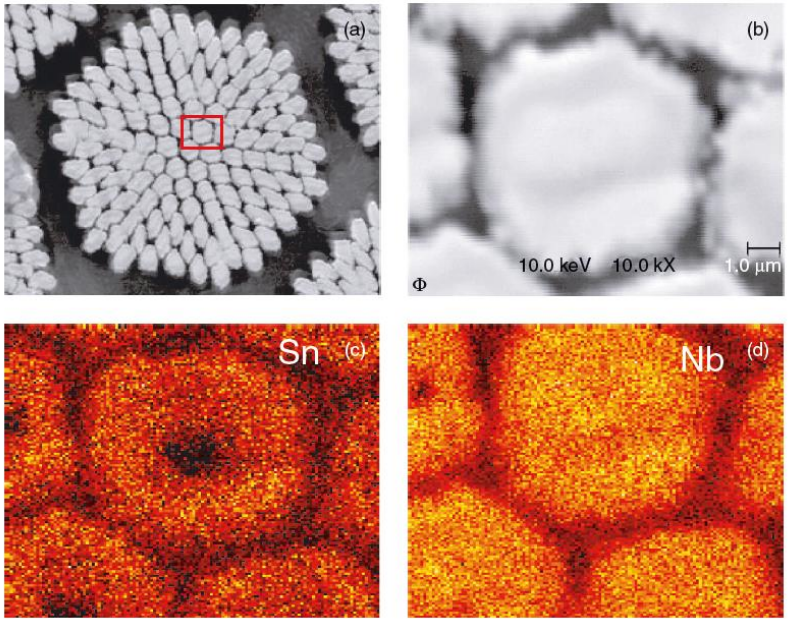

Figure 2.20 AES mapping – scanning Auger micrographs of an Sn–Nb superconductor multi-wire: (a,b) SEM, (c) Sn and (d) Nb elemental distributions

The line-scan profile and mapping image shows the peak intensity of each pixel with high lateral resolution.

J. C. Vickerman, Surface Analysis-The principal Techniques, 2nd Ed., John Wiley & Sons, Ltd., 2009, p. 27, p. 28

AES Depth profiling

– With the anodized sample, the Cu/Ni ratio is almost zero for the first 10 minutes (for depth of about 50 nm). The ratio then rises and approaches that for a bulk sample of alloy.

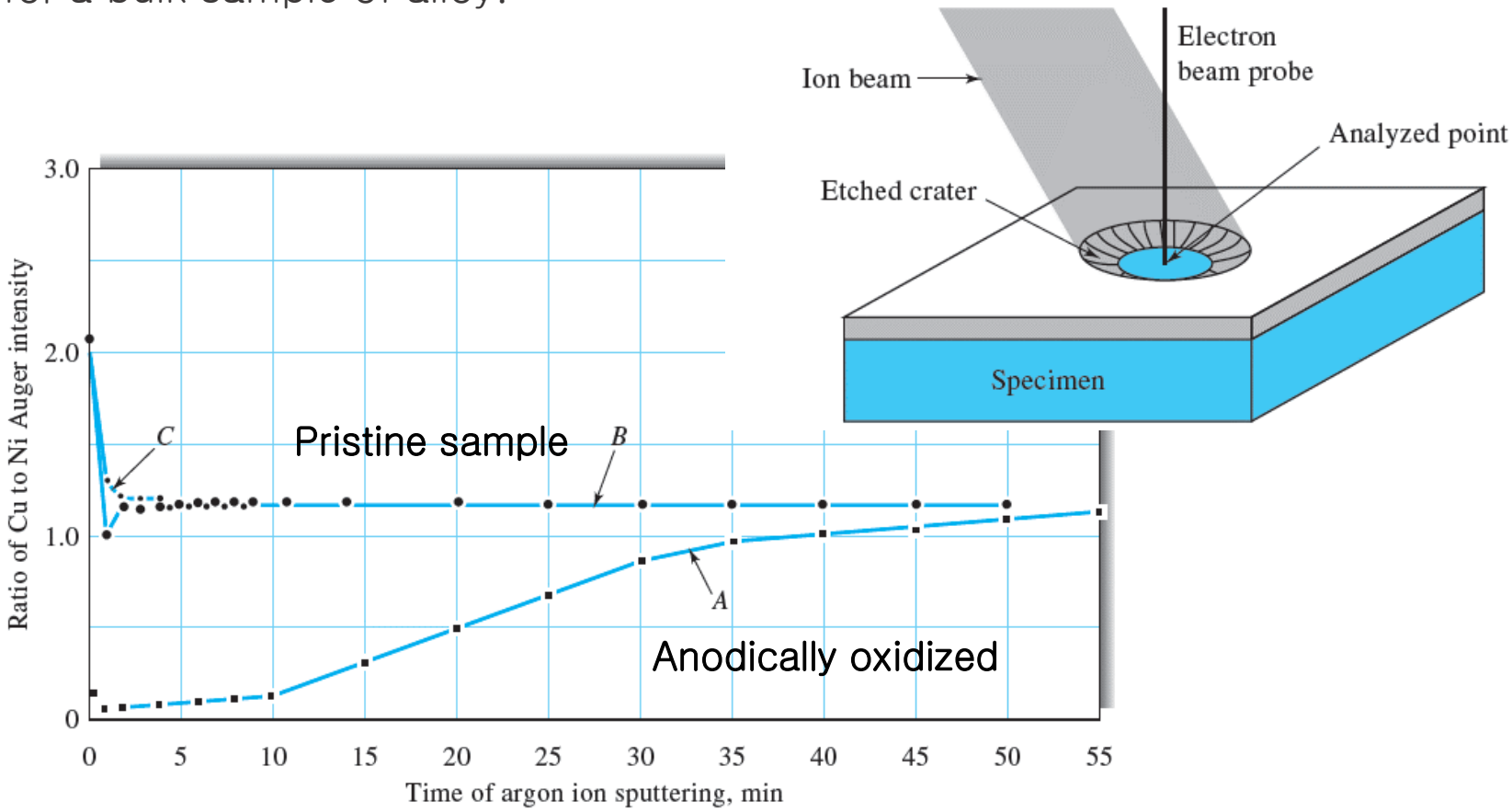

FIGURE 21-11 Auger sputtering profiles for the copper-nickel alloys shown in Figure 21-8: *A*, passivated sample; *B*, nonpassivated sample; *C*, chemically etched sample representing the bulk material. (Adapted from G. E. McGuire et al., *J. Electrochem. Soc.*, **1978**, *125*, 1801, **DOI:** 10.1149/1.2131298. Reprinted by permission of the publisher, the Electrochemical Society, Inc.)

D. A. Skoog, Principles of Instrumental Analysis, 7th Ed., Cengage Learning, 2017, pp. 547-548